Addis Ababa University
አዲስ አበባ ዩኒቨርሲቲ
Seek Wisdom, Elevate your Intellect and Serve Humanity

SCHOOL OF EARTH SCIENCES

GEOPHYSICAL MAPPING OF THE GROUNDWATER AQUIFER SYSTEM IN GODE AREA, NORTHEASTERN HOSANNA, ETHIOPIA

A THESIS SUBMITTED TO THE SCHOOL OF GRADUATE STUDIES OF ADDIS ABABA UNIVERSITY IN PARTIAL FULFILLMENT OF THE REQUIREMENTS FOR THE DEGREE OF MASTER OF SCIENCE IN EARTH SCIENCES (GEOPHYSICS)

BY

ESUBALEW YEHUALAW

ADDIS ABABA UNIVERSITY

ADDIS ABABA, ETHIOPIA

JUNE, 2020

ADDIS ABABA UNIVERSITY

SCHOOL OF GRADUATE STUDIES

This is to certify that the thesis prepared by **Esubalew Yehualaw**, entitled **"Geophysical Mapping of the Groundwater Aquifer System in Gode area, northeastern Hosanna, Ethiopia",** submitted in partial fulfillment of the requirements for the degree of Master of Science in Geophysics complies with the regulations of the University and meets the accepted standards with respect to originality and quality.

Approved by board of examiners:

	Signature	Date
Dr. Balemwal Atnafu (Head, School of Earth Sciences)	_____	_____
Prof. Tigistu Haile (Advisor)	_____	_____
Dr. Abera Alemu (Internal examiner)	_____	_____
Dr. Dessie Nedaw (External examiner)	_____	_____

DECLARATION

I, the undersigned, hereby declare that the thesis entitled with **"Geophysical Mapping of the Groundwater Aquifer System in Gode area, northeastern Hosanna, Ethiopia**" is my original work carried out under the supervision of Professor Tigistu Haile. The thesis has not presented to any university or institution for the award of any degree or diploma and all sources of materials used for the thesis are duly acknowledged.

Name of the candidate	Signature	Date
Esubalew Yehualaw	_____	_____

This is to certify that the above declaration made by the candidate is correct to the best of our knowledge and it has been submitted for examination with our approval as university advisor.

Prof. Tigistu Haile	Signature	Date
(Advisor)	_____	_____

ABSTRACT

In this study, the basic geophysical methods are applied for mapping the groundwater aquifer system in Gode area along the Guder River, northeast of Hosanna town, near the western margin of the Central Main Ethiopian Rift. The need for additional water resources in Hosanna town and its surrounding area is highly increasing due to the growth of the population over time and the expansion of irrigation activity. This study is aimed at mapping the potential aquifer zone and investigates the groundwater potential for the current and future development of the resource at Gode area.

Geophysical methods employed in this study include, Vertical Electrical Sounding (VES) and magnetic survey techniques. Electrical sounding was used to examine and map the depth to the potential aquifer zone of the groundwater and its distribution over the area. On the other hand, magnetic survey was used to delineate contact between lithologic units and geological structures, which control the groundwater flow and storage system. The geophysical survey comprises of twelve VES readings by using Schlumberger array along six profile lines and more than four hundred (400) magnetic readings at about 10m station interval along four profiles and 20m along three random profiles.

Information from nearby boreholes were integrated to constrain the resistivity sounding survey with geological layers and various types of magnetic data plots and 2D magnetic models to enhance and visualize the results. The results of the geophysical survey are presented in the form of interpreted VES curves, pseudo depth and geoelectric sections, sliced and sliced-stacked maps, magnetic anomaly plots and 2D model section. The study result revealed that the potential aquifer in the area is obtained at depth range from 45m to 92m. This is the response of the highly weathered/ fractured ignimbrite and pumice layer with sandy soil, which is the main water-bearing horizon. Overall, in the neighborhood of four VES points, VES- 2, VES- 3, VES-10 and VES-11, shows good water bearing zones in the study area.

Keywords: Vertical Electrical Sounding, Magnetic survey, Aquifer, Groundwater Potential, Water table

ACKNOWLEDGEMENT

Without the help of many people and organization, compilation of this thesis would not be possible. I would like to take this opportunity to express my appreciation to everyone assisted in one-way or another. Greatest appreciation goes to my advisor Professor Tigistu Haile for his invaluable assistance during my study and constructive guidance all along from the fieldwork to the completion of the research. His continuous support, advice, discussion and suggestions guide me to become a self-reliant.

I would like to thank my instructors' Professor Tilahun Mammo, Dr. Abera Alemu, Dr. Atalay Ayele for their provision of reliable knowledge and information during learning of geophysics.

My warmest gratitude also goes to my best friend Tekalgn Beyene who helped me for his support and encouragements since the begging of the study. I am grateful to all graduate students of the geophysics stream for discussion and encouragement for the success of this M.Sc. thesis work. Especially, Wubayehu Desalegn for her support and devote much of time and energy during field data collection.

I am also thanks to Hadiya water work design and supervision enterprise Bureau where I got the lithologic log data and geological reports of the study area.

Last but not least, my deepest gratitude goes to my Family particularly, my brothers Abebe Yehualaw and Nigussu Yehualaw for their persistent moral support and encouragement during my study. Their tolerance and patience have contributed a lot towards a successful completion of my studies. This without their assistance would have been much more difficult. Once more, I want to extend my appreciations and thank to my friend Wubamlak Nigussie for his support the beginning to the end.

TABLE OF CONTENTS

LIST OF FIGURES

LIST OF TABLES

LIST OF ACRONYMS

1D	One Dimensional
2D	Two Dimensional
BH	Borehole
CMER	Central Main Ethiopian Rift
DW	Dag Well
EIGS	Ethiopian Institute of Geological Survey
GPS	Global Position System
IGRF	International Geomagnetic Reference Field
MER	Main Ethiopian Rift
m	Meter
ms/cm	Micro Siemens Per Centimeter
NS	North-South
NW	Northwest
nT	Nanotesla
SE	Southeast
NE	Northeast
SI	Structural Index
TMI	Total magnetic intensity
Ω-m	Ohmmeter

CHAPTER ONE

INTRODUCTION

1.1. General Background

Water is the basic component of life and the central part of all efforts to address food security, economic growth and energy production (Gebremedhin Breanne et al., 2015). According to these and other related studies, for any developmental activity, both surface and groundwater resources are the main components depending on their quality and availability. With time, due to population growth and the expansion of irrigation activity the use and sustainability of water resources have become scarce (Farrag et al., 2002). Therefore, it is of great importance that water resources of an area should be developed and used in a sustainable manner to maintain adequate water supply and preserve the environment for availability of groundwater resource.

Groundwater is one of nature's valuable resources for life and it is a crucial source of fresh water over the world (Haile Arefayne and Semir Abdi, 2016). It is that portion water arising from atmospheric precipitation, mostly rainfall, which has percolated into the Earth to form underground deposits in horizons referred to as aquifers, which are geologic/ lithologic units (Yousef et al., 2015). According to Srinivasa, et al., (2000); Vijith, (2007) the occurrence and movement of groundwater, especially in fractured bedrock aquifers in a given area, is governed by many factors such as topography, geological structures, fracture density, secondary porosity and climatic conditions.

Based on the studies given by Farrag et al., (2019) the amount of groundwater in the subsurface is mainly dependent on the permeability of rock materials. According to their studies, the permeability of material is grouped into two and these are: permeable layer (sand, gravel, unconsolidated, fractured or weathered rocks) and impermeable or semi-permeable layer (clay, consolidated sediments or solid rocks).

Tenalem Ayenew et al., (2008) also analyzed the occurrence and distribution of groundwater aquifers in Ethiopian depend on various environmental and geological factors.

As a result, of these variations in rock type, the groundwater potential varies from place to place, sometimes within a few meters and even within the same geological formation (Imran et al., 2010).

According to Yousef et al., (2015) there are several methods employed for delineating groundwater potential zones; these include geological, hydrological, geophysical and remote sensing techniques. However, the advantage of geophysics for both groundwater resource mapping and for water quality evaluations has increased dramatically over the last few decades (Sultan, 2016). The main reason for this is that the use of geophysics for groundwater studies has been inspired in part by a desire to reduce the risk of drilling dry holes.

Currently, the geophysicist also provides useful parameters for hydrogeological modeling of both new groundwater supplies and for the evaluation of existing groundwater depletion and contamination. In this respect, the major perspective of this study is to identify the potential of the aquifer system at Gode area along the Guder River, near Hosanna town in the southern region of Ethiopia for extraction of groundwater resources and minimize the risk of sinking dry boreholes at inappropriate locations using geophysical techniques. Specifically, this is planned to be achieved by obtaining information on the presence and subsurface distribution of aquifers and controlling geologic structures using the Vertical Electrical Sounding (VES) and magnetic methods of prospecting. According to Shaaban, (2002) the electrical resistivity of a formation is mainly dependent on the salinity of its fluid content, saturation, aquifer lithology and porosity.

Some or most of these parameters determine the resistivity of formations in the subsurface that could be measured with the VES technique. On the other hand, the magnetic method is employed to map contact between lithlogic units that are suitable for groundwater accumulation and assess the potential zones of groundwater saturation through delineation of fractures and faults in the study area so as to govern the flow and movement of groundwater (Israil et al., 2006).

The main goal of this study was to gain a better investigation of groundwater potential problem with respect to its aquifer character by using resistivity and magnetic method for enhanced the development of groundwater in the area.

1.2. Description of the Study area

1.2.1. Location and accessibility

Hosanna town is a part of the Southern Nation Nationalities and People's Regional State (SNNPRS) of Ethiopia, situated in Hadiya Zone; and is located 230km away from Addis Ababa. It is geographically located at 833500 North and 372100 East longitude with an elevation of 2,177 meters above sea level. Specifically, the town is found at the western margin of the Main Ethiopian Rift (MER) that runs from northeast to southwest almost dissecting Ethiopia into two parts. The specific study area, Gode, is located northeast of Hosanna town about 8.4km and 2km from Belesa town. The main asphalt road from Addis Ababa to Hosanna crosses the northeast part of the study area. The area to the potential well field is also accessed, by detouring from the main asphalt road in a southeast direction and moving for about 1km on a standard gravel road to the crossing of Guder River (Figure 1.1).

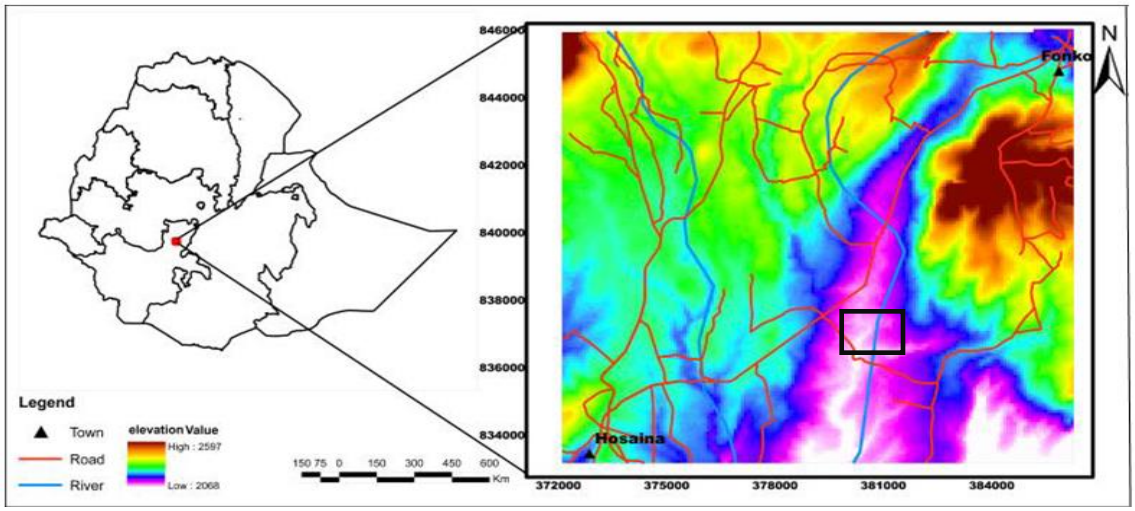

Figure 1.1 Location map of the study area (Rectangle in black color).

1.2.2. Physiography and Drainage Pattern of the study area

Most part of Lemo Woreda, especially Belesa and Lisana areas are categorized as the transitional escarpment zones with altitude ranges of 2,150 – 2,180m above mean sea level. The physiography of the study area is generally, characterized by a dendrite drainage pattern along the Guder River cuts, The drainage pattern of the study is also observed to be highly

controlled by structures, which occupy weak zones mainly exposed in the quarry site of northeast and southwest part of the survey along the Guder River (Figure 1.2).

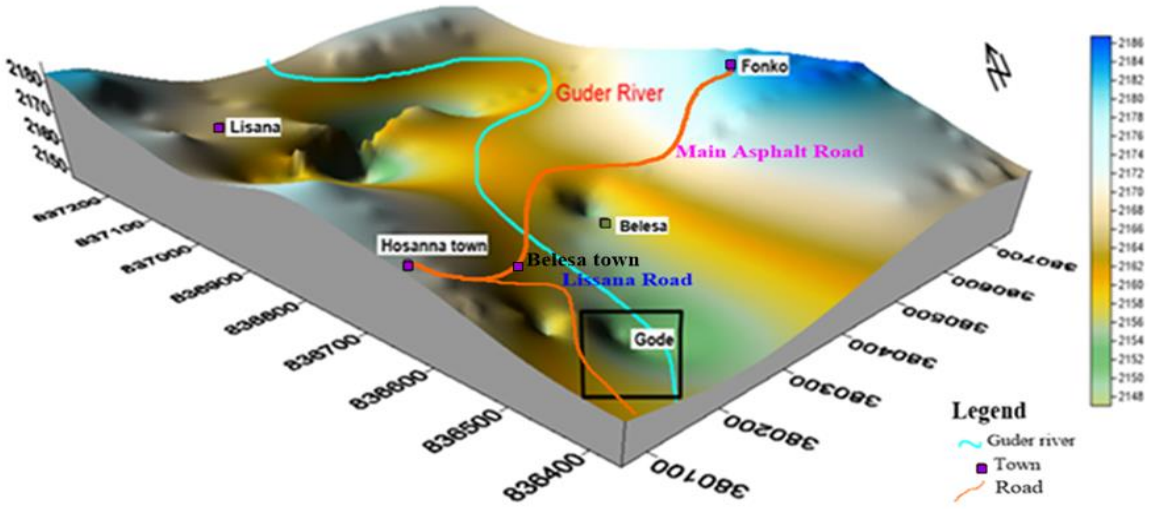

Figure 1. 2 Physiography map of the study area and its surrounding area, (the black rectangular shape indicates the current targeted area).

1.2.3. Climate and Vegetation

According to "climate-data.org" in https://en.climate-data.org/location/3664/ the area is characterized by a warm and temperate climate and gets a major rainfall even during the winter season. The average temperature and precipitation of Hosanna town and its surrounding area is as described as in the Figure 1.3. It is seen that from the (Figure 1.3) that the area records highest average temperature of 18.6^{o}C in March, whereas, the lowest average temperature measured in August is about 15.8^{o}C. The wettest month (August) measures the highest precipitation (167mm) while the lowest precipitation is record in December (17.5mm).

1.2.4. Land Use/ Land Cover

Topography and soil types govern land use activity of the study area. The central portion of the area forms a gentle slope and thick soil cover due to weathering of Guder River. Almost all of the study area is covered by farmland used for agricultural products such as Wheat, Maize, Teff, Sorghum and partially for grazing land for cattle's.

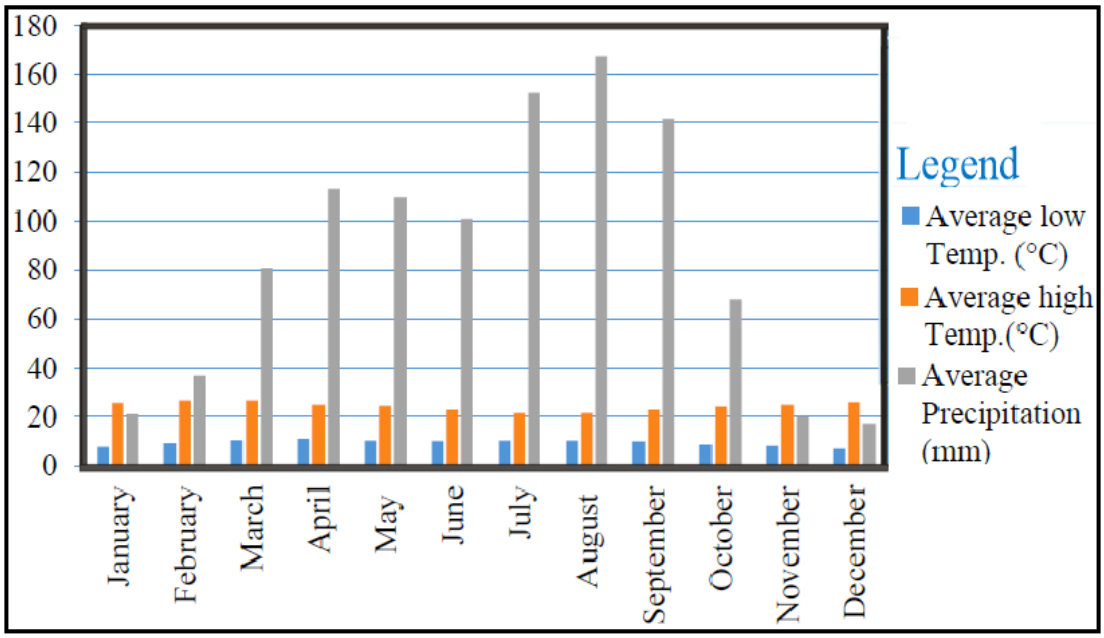

Figure 1. 3 Temperature and precipitation of Hosanna and its surrounding **(https://en.climate-data.org/location/3664/)**

1.3. Objectives

1.3.1. General objective

The main objective of this work is to map the groundwater aquifer zones and determine the groundwater potential of Gode area, near Hosanna town using a combination of geophysical techniques namely, electrical resistivity and magnetic methods of prospecting.

1.3.2. Specific objectives

The following are the specific objectives of this research

- To map subsurface layers and their thickness in view of their potential to act as a good groundwater potential zone;
- To identify the distribution of major water bearing/ aquifer formations and their depth over the area of the study;
- To map subsurface structures, contact between lithlogic units and weak zones that could play a great role in groundwater movement and accumulation;
- To locate and delineate possible potential sites of groundwater development;

1.4. Problem statement

In most southern region of Ethiopia, especially in Hadiya Zone, groundwater has a paramount importance for primary domestic supply, agriculture and industrial use. However, Hadiya Zone has been frequently affecting by recurrent drought due to scarcity of rains and as a result the population is not food secure; this is typically so in Lemo Woreda. Hosanna and its surrounding areas are currently getting their water supply from boreholes and motorized springs found within the different parts of the current study area around Guder River.

About six boreholes that have been drilled to different depths exist in parts of the area supplying water to Hosanna town and the surrounding communities. Even though these boreholes are drilled in close proximity to Guder River for extraction of this resource, besides to a study on the sitting of these existing wells, there is no detailed geophysical investigation that has been conducted to understand the groundwater potential of the Guder River course and its surroundings.

Consequently, the exploration for groundwater done so far is not adequate to solve the problem in relation to the demand for clean water that is continuously raised in the society. Moreover, some of the existing boreholes are currently non-functional due to unknown problems making the water scarcity even more acute. Now, the need for additional water sources in Hosanna town and its surrounding rural areas is highly increasing due to the growth of the population over time and the expansion of irrigation activity.

Therefore, the main intention of this study on the survey part of Gode area is to identify the potential aquifer zone and investigate the groundwater resource for the current and future development.

1.5. Review of the previous works

Many authors (geologists, hydrogeologists and geophysicists) have conducted surveys and implemented mapping techniques to investigate and give more information about the groundwater potential in different zones with their lithological, hydraulic and petrophysical characteristics of the studied areas (Farrag et al., 2002; Elewa, 2008; Yousef, 2008; 2015; Bitsiet Dereje and Dessie Nedaw, 2019; Sultan, 2019).

Nowadays, most Ethiopian hydrogeological studies have been carried out to achieve a better picture of the hydrology of major river basins leaving a big information gap in the hydrogeology and groundwater of specific area (Tenalem Ayenew, 2001; Tamiru Alemayehu, 2006). In their studies, they describe the most important source of groundwater, potential recharge and the distribution of lithologic rock units in Ethiopia.

Some authors used different geophysical tools such as magnetic and resistivity for groundwater exploration (Sultan, 2019; Araffa et al., 2017) studied the infiltration capacity and groundwater potentiality of the respective area of study. Amongst those, a few authors have discussed the theory and application of the resistivity method and great variations in success have been noticed. According to the studies of Flathe, et al., (1970) the geoelectrical technique is the most effective method for groundwater exploration in order to correlate between the electrical properties of the geologic formations and their fluid content.

A number of studies have described the advantage of electrical resistivity method in groundwater exploration (Young et al., 2008; Lashkaripour et al., 2005; Hassanein et al., 2007). According to these studies, the authors summarized that the electrical resistivity technique is widely used to estimate the depth and the nature of the alluvium, aquifer boundaries and its location. Furthermore, the electrical resistivity method has also been used to delineate the fresh water/ saline water interface (Yechieli, 2000; Choudhury et al., 2000; Shaaban, 2002).

Recently, the electrical resistivity method is the most effective technique to identify the aquifer porosity (Jackson et al., 1978), hydraulic conductivity (Yadav and Abolfazli, 1998; Troisi et al., 2000), transmissivity (Kossinski and Kelly, 1981) and groundwater contamination zone (Kaya, 2001).

The other most effective advanced method is the magnetic survey, which has been widely used in groundwater exploration where delineating structures was the main target (Hassanein et al., 2007).

1.6. Methodology

The geophysical techniques utilized in this research work are the magnetic and electrical resistivity methods. The application of these combination of methods is conducted through a

number of different consecutive steps of desk study, method selection, field survey design, data collection, data analysis and interpretation to achieve the final set goals.

Initially, relevant literature was reviewed in order to have a general overview about geological and hydrogeological aspect of the study area and its surrounding regions. This part of the study provides important information about the area, what other authors did and recommended earlier in terms of determining the data gaps. Further, before the geophysical survey, it is essential to conduct desk studies, collect secondary data from various organization and physical field observations in order to make geophysical studies more targeted and effective.

The next phase involves geophysical data acquisition, processing and interpretation in light of existing background information harvested from the initial phase. The geophysical methods of investigation employed, as mentioned in the previous sections, were the electrical resistivity and magnetic prospecting. The resistivity and magnetic data were collected along selected profiles.

After returning from the field, all geophysical data have been corrected, analyzed and data syntheses were conducted to process the raw data using different geophysical software and computer applications. Specifically, the software that are used included: - MS Excel, Surfer, WinResist, RESIXIP, Oasis Montaj, AutoCAD, and Corel Draw and others.

Using a combination of these, geophysical maps and plots are produced and the correlation between the results of the two geophysical methods employed and geological information was made. Maps and plots are interpreted to give geological meaning, which leads to the discussion and conclusion about the result. The above objectives are believed to have been reached properly and timely by using these appropriate methodology and steps.

The most important outcome of the study is locating and selecting the appropriate location of potential borehole sites for drilling to tap the subsurface saturated zones. Finally, information regarding geological, hydrological and geophysical input gathered from the field as well as from different sources including hydrogeological borehole logs was used to produce the final report. The methodology and steps followed to conduct this research is presented in the flow chart given in Figure 1.4.

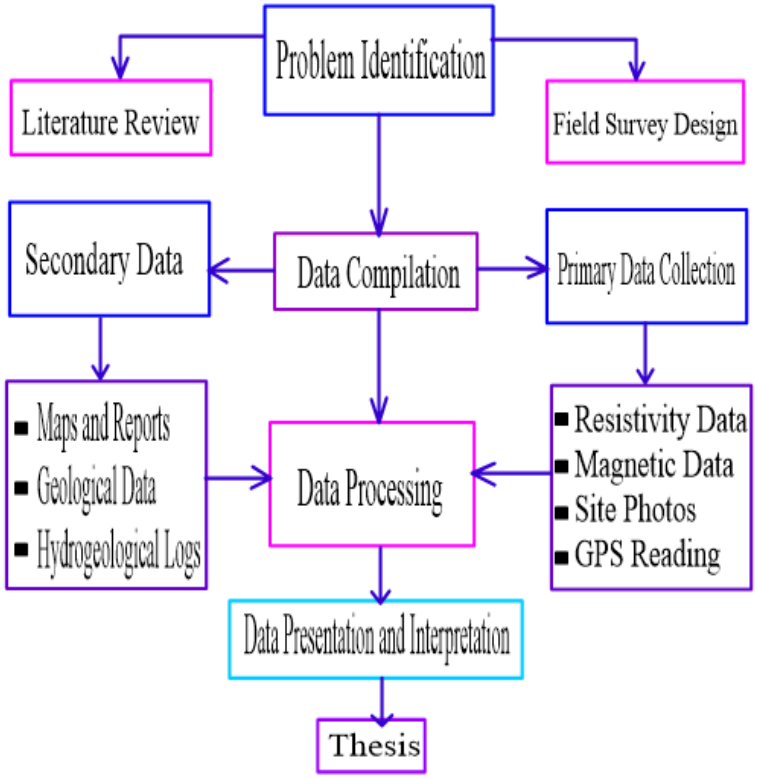

Figure 1. 4 Flow chart of methodology used in the current research work.

1.7. Significance of the study

The main significance of the output of this research project is particularly produce a better understanding of the groundwater potential and aquifer characteristics of Gode area near Hosanna town. It is significant in that it mapped structures (such as fault, and weak zones) and has defined the geological stratification of the study area in view of their suitability for groundwater saturation, storage and potential for exploitation.

In addition, this research project has made analysis on the role of groundwater flow system in the subsurface layer of the study area. In summary, the study has the following significances:

- It provides information about the hydrogeology, aquifer zone, its depth as well as the drilling point of high potential zone of groundwater in the study area.
- This research work fills the existing gap of detail information and can solve the scarcity of water in the Gode area.
- It gives some initial information for future detailed study in the area, which leads researchers for further research activity.

1.8. Limitation of the study

Like any other research works, this study has faced a number of limitations. The major problems that were encountered during the research study are scarcity of previous geophysical data, difficult terrain for VES survey, problems associated with right of way (permission to work) on the area.

1.9. Structure of the thesis

This M.Sc. thesis work is divided into six (6) Chapters. The first chapter is general introduction of the study, which includes description of the study area, statement of problem, objectives, methodology and review of previous works. The second chapter is concerned mostly with previous studies that includes local and regional geology and hydrogeology of the study area and its surroundings. The third chapter presents the theoretical background of the geophysical methods of investigation employed in the research work. The fourth chapter deals with data acquisition, processing and presentation of the VES, and magnetic data. The fifth chapter deals with the discussions and interpretation of the processed and presented data or the results of the work. The last chapter, chapter six, deals with the conclusions and recommendations of the study based up on the result.

CHAPTER TWO

GEOLOGICAL AND HYDROGEOLOGICAL SETTING

2.1. Geological Setting

2.1.1. Regional Geology

The Main Ethiopian Rift is a magmatic rift that recorded all the different stages of rift evolution from rift initiation to break up and incipient oceanic spreading (Ebinger, 2005; Corti, 2009). The Main Ethiopian Rift is divided geographically into three sectors: northern, central, and southern MER (Gidey Wolde Gabriel et al., 1990). The study area is the part of the Central Main Ethiopian Rift (CMER), which found the western side of the Main Ethiopian Rift.

Tsegaye Abebe et al., (2010) the Main Ethiopian Rift (MER) is bounded by discontinuous boundary faults that give rise to major fault escarpment separating the rift depression from the Somalian and Ethiopian plateaus. In addition, it is bounded by the Goba- Bonga lineament to the Yerer-Tullu- Wellel and to the west by Guraghe fault escarpments (Figure 2.1). According to Tsegaye Abebe et al., (2010) the Central Main Ethiopian rift is mainly covered by a volcanic rock, where the area exists basalts, felsic-volcanic rocks (ashes, tuffs, pyroclastic rocks, trachyte and rhyolite) and re-deposited fluvio-lacustrine sediments. Those volcanic rock litho types can release weathered chemical components into interacting water. As a result, the suitability of groundwater for water resource use in the rift is poor discharged which includes high salinity and high fluoride contents (Tenalem Ayenew, 2008; Seifu Kebede, 2010).

The geological setting of central Ethiopia is classified in six lithological units (Tsegaye Abebe et al., 2010).

1. Pre- Tertiary sediments and crystalline basement

The regional faults expose basement rocks beneath tertiary volcanic rocks in the southern sector of MER, however in the central and the northern sectors, the rift margins are Tertiary silicic and mafic rocks. Pre- Tertiary crystalline basement and Mesozoic sedimentary rocks

are overlying by Oligocene basalt flows are exposed in the western margin of the central sector at the Guraghe Mountains (Gidey Wolde Gebriel et. al., 1990).

2. Oligocene and lower Miocene plateau volcanic

This is the oldest volcanic unit in the central sector of the MER and is found at Ambo and Agereselam, and Welkite shield volcano. Gidey Wolde Gabriel et al., (1990) suggested the average thickness at Guraghe margins 600-700m. For both volcanic events, widespread time-correlative basaltic units occur on the western and eastern margins of the central MER.

3. Miocene-Pliocene rift-shoulder trachytic-rhyolitic volcanics and pyroclastic layers

Several layers of the pyroclastic units associated with rhyolitic lava domes and flows together with some important central volcanoes were formed in this episode, and cover the MER shoulder floor. This episode consists of un compacted pumiceous fall and flow deposits, fissural basaltic lava flows with associated scoria and interbedded lacustrine deposits (Kazmin, 1980).

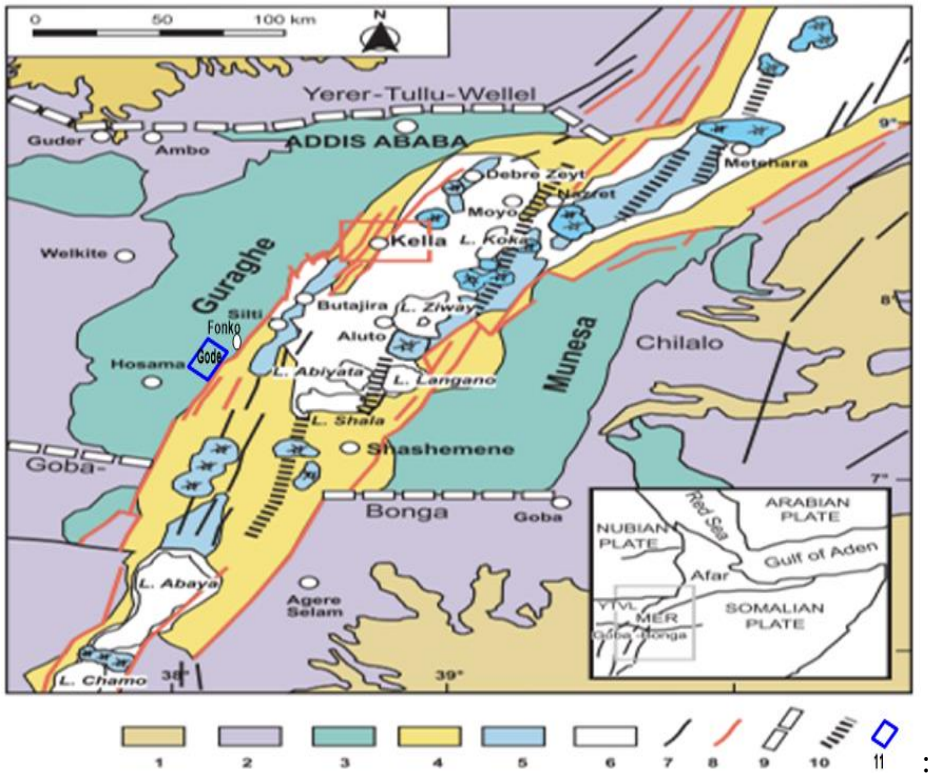

Figure 2. 1 Geological map of central main Ethiopian rift (Tsegaye Abebe et al., 2010)

(1) Pre-Tertiary sediments and crystalline basement, (2) Oligocene (32-29Ma) and lower Miocene (12-8 Ma) plateau volcanics, (3) Miocene-Pliocene rift-shoulder trachytic-rhyolitic volcanics and pyroclastic layers, (4) Plio-Pleostocene rift floor, (5) Quaternary central volccanics and basaltic lava flows, associated scoria cones and phreato-magmatic deposits, (6) Quaternary lacustrine sediments and interbedded pyroclastics, (7) Faults, (8) Major rift border faults, (9) Major transversal tectonic lineaments in the basement, (10) Wonji Fault Belt segments: Red square area show Kella area. YTVL refers Yerer-Tullu-Wellel volcano tectonic lineament, (11) the targeted area.

4. Plio-Pleistocene rift floor

Volcanic rocks of Pliocene age such as rhyolite, trachytes, ignimbrites and basalts are abundant within the rift floor (Kazmin, 1980). Silcic pyroclastic materials cover most of the MER floor, they are mainly paralkaline rhyolitic ignimbrites intercalated with basalt and tuff (Gidey WoldeGebriel et al., 1990).

5. Quaternary central volcanics and basaltic lava flows, associated scoria cones and phreatomagmatic deposits.

Tsegaye Abebe et al., (2005) have carried out the Quaternary volcanic setting was spatially associated with the Oblique faults of the Wonji Fault belt affecting the rift floor and still characterized by both silicic and basalts (Rhyolites and Wonji Basalt).

6. Quaternary lacustrine sediments and interbedded pyroclastics

Bimodal volcanic rocks (lava, pyroclastics and volcanoclastic strata) in the quaternary (<1.6-1.8Ma) were generally closely associated with Wonji Fault Belt affecting the rift floor (Gidey WoldeGebriel et al., 1990). In the rift floor, interlaying of air fall pyroclastic deposits and lacustrine deposits are common (Kazmin et. al., 1980).

2.1.4. Local geology of the study area

The study area is covered by thick soils, except at river cuts and road sections where extensive exposures of the rock units are visible. Cenozoic (young) volcanic rocks and thick residual deposits characterize the area. Local geologic setup of the study area was described

based on the observations of river cut, road section, quarry sites, boreholes and drainage network patterns and is as shown in the Figure 2.2.

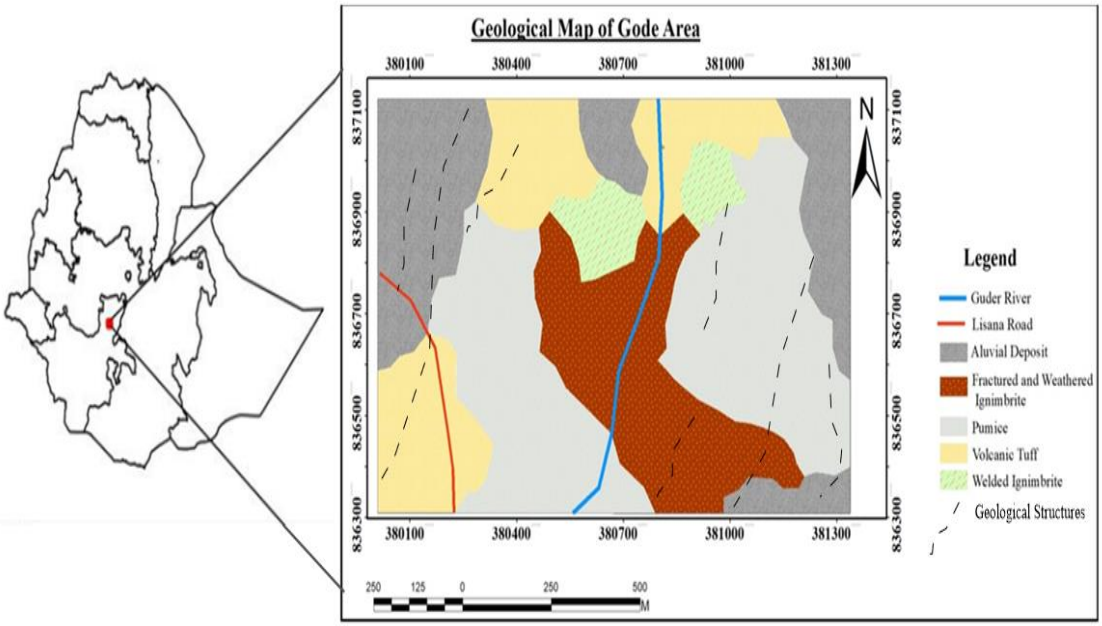

Figure 2. 2 Geological map of Gode area, the study site.

The geological units of the study site are ignimbrite, pyroclastic ash tuff, volcanic ash and residual soils. The brief descriptions of these different units are as follows:

Ignimbrite: it is welded tuff and a special group of pyroclastic rocks. It is found exposed along the Guder River cut in the northern and southern portions of the study area. Fresh ignimbrite deposits are characterized by poorly sorted aggregates of tuff and pumice. The weathered and highly fractured ignimbrite is found in the southwestern portion of the study area (Figure 2.3). It is intercalated with reddish clay soil and tuff in many parts of river exposure. The intercalation shows depositional series of pyroclastic materials.

Pyroclastic ash tuff: it is well- sorted and fine to medium grained. This pyroclastic unit is exposed in the eastern, western and southern portions of the study area along river cuts and road sections. It is characterized by white color and fine-grained texture (Figure 2.4). The tuff unit of the study area is relatively soft and porous that is usually formed by the compaction and cementation of volcanic ash.

Figure 2. 3 Fractured and weathered ignimbrite with collapsed pumice found in the southern part of the study area.

Figure 2. 4 Pyroclastic ash tuff and pumice at quarry site exposures.

2.2. Hydrogeological Setting

According to Tenalem Ayenew et al., (2008) hydrogeological conditions of the permeable rocks and high recharge rate are mainly controlled by the lithologies, geological structures and geomorphology. The groundwater reserve in rocks is low due to the fast release of the recharged water to the rift plains through large open faults (Tenalem Ayenewet al., 2008; Bitsiet Dereje and Dessie Nedaw, 2018). Previous studies (Fitter, 1994) have investigated and concluded that the groundwater inevitably occurs in geological formations and one requires information on how these Earth materials are formed and the changes they have undergone in order to better understand the allocation/ distribution of geological structures.

In addition, Seifu Kebede, (2010) also described that groundwater circulation and storage in the volcanic rocks depends on the type of porosity and permeability formed during and after the rock formation. Littman, (1964) have discussed the probability of obtaining high yield wells in crystalline rock areas, if drilling takes place in an area where fractures are localized.

Though porosity may be high, permeability which is largely dependent on the primary and secondary structures of the rock mass affects the yield of wells in such situations (Tenalem Ayenew and Tamiru Alemayhu, 2001). The intermountain grabens and rift floor sediments associated with fractured volcanics form the largest aquifers under water table and semi-confined conditions presented by Tenalem Ayenew et al., (2008).

Therefore, acquiring knowledge about the existing of aquifer materials and information on their geological setting is necessity. The map in (Figure 2.5) shows the hydrological setting of the study and its surrounding area.

2.2.1. General description of the aquifer system in the study and surrounding area.

An aquifer is a rock that holds or transmits water to wells and springs in useful or economic quantities (Todd, 2004; Seifu Kebede, 2010). According to EIGS, (1993) two major aquifer classes were identified in the Ethiopian Rift based on the mode of origin and the rock types. These are (1) extensive aquifers with intergranular permeability (unconsolidated sediments: alluvium, and lacustrine sediments) and (2) extensively fractured and weathered volcanics (basalts, rhyolites, trachytes and ignimbrites).

The most important aquifers are thick pyroclastic deposits, volcanic rocks within structural discontinuities in the rift and escarpments, which provide the best aquifer materials defined by (EIGS, 1993).

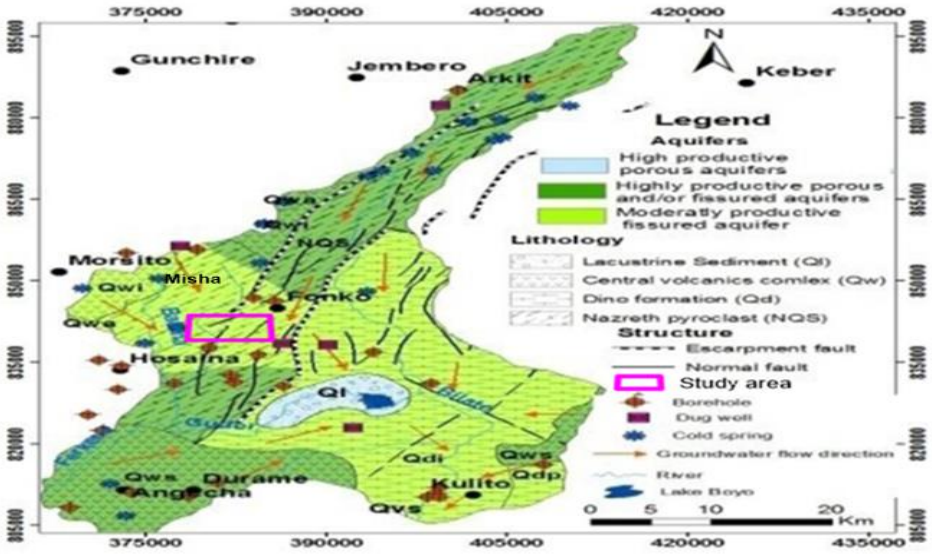

Figure 2. 5 Hydrogeological map of the area, area marked with rectangle is the specific study area (from Bitsiet Dereje and Dessie Nedaw, 2018).

According to Tenalem Ayenew et al., (2010) the following aquifer/ aquitard were defined.

2.3. Hydrogeology and Aquifer Type of the Study Area

The hydrogeology of the area shows aquifers and aquitards defined based on the character of the groundwater flow (pores and fissures), the yield of springs and the hydraulic characteristics of boreholes. Common aquifers are geological formations of unconsolidated sand and gravel, sandstone, limestone and fractured volcanic rocks. Examples of common aquitards are clays, shales and silt (Seifu Kebede, 2010).

2.3.1. Extensive and Moderately Productive Porous and/or FissureAquifers

Quaternary volcanic rocks like scoria basalt, weathered and fractured ignimbrites have dominant fissured permeability and represent porous aquifers of the area. According to Sintayehu Legesse, (2009), the western part of highland areas including Lisana and Angacha Woreda have relatively high precipitation and are categorized as moderately productive aquifers.

2.3.2. Local and Moderately Productive Fissured Aquifer

Permeability is largely a function of the primary (porosity) and secondary structures (joints and fractures) within the rock. Welded ignimbrites usually alternate with non-welded ones and are intercalated with tuff, pumice and lacustrine sediments. Including some parts of Gode and Belesa in the neighborhood of the study area have relatively low to moderate aquifer.

2.3.3. Formation Consisting of a Minor Fissured Aquifer-Aquitard

Aquitards are unites where groundwater is neither stored nor transmitted, i.e. and there is minimal flow through the rock. It is hard to get shallow wells in Misha Woreda and some part of Lemo Woreda due to less fractured rocks, as presented by (Sintayehu Legesse, 2009).

CHAPTER THREE

THEORETICAL BACKGROUND OF THE GEOPHYSICAL METHODS OF INVESTIGATION

3.1 General

Geophysics is the scientific method that uses the science of physics with high degree of technological development employed to observe the hidden subsurface of the Earth (Kearey and Brooks, 2002). The theoretical background of geophysics has been extensively reviewed by many authors (see the classical texts Dobrin, 1976) and can be studied in the standard texts such as that by Telford et al., (1990). Today, several studies have proved geophysical methods as a powerful tool in the detection of groundwater contaminants and have also been used to characterize gas-phase dynamics in groundwater investigation; (see for example Brewster et al., 1995).

For groundwater investigations, the most significant parameters that have been used to describe an aquifer system are the ones that relate to the porosity and permeability of the aquifer and the surrounding aquitard (Mazac et al., 1985). Most geophysical techniques have been used for groundwater characterization but once again, it is with the electrical and magnetic methods that the greatest success has been shown in directly mapping and monitoring the contamination of clean groundwater. Accordingly, these two methods have been used for groundwater potential assessment and aquifer characterization over the area which is the subject of this study, i.e., at Gode- an area in close proximately to and along the Guder River, northeast part of Hosanna. The theoretical foundations of the methods are therefore, briefly discussed in the following sections.

3.2. The Electrical Methods

Electrical methods of geophysical prospecting are well established and are the most important methods for groundwater investigation, because it is the best method to detect the existence between electrical properties, geologic formations and their fluid content (Flathe, 1955; Zohdy, 1969; Flathe, 1970; Zohdy et al., 1974). The advantages of electrical methods also include control over depth of investigation techniques, portability of the equipment,

availability of wide range of simple and elegant interpretation techniques. Different authors, Telford et al., (1990) are described the theory and basic principle of electrical resistivity method. Electrical method of groundwater survey is based on electrolytic conduction, where four metallic electrodes are coupled to the ground and connected to the resistivity meter through conducting wires (Figure 3.1). The two outer electrodes A and B introduce current to the rock formation; the two inner electrodes M and N measure the potential difference.

3.2.1. Equipment of Electrical Resistivity Survey

The basic equipment required for the electrical resistivity survey consists of a transmitter, a receiver, steel electrodes, hammer, connectors, field work sheet of note pad, current and potential wires are shown in (Figure 3.1).

Figure 3. 1 Equipment layout for electrical resistivity survey (Image extracted from http://pasisrl.en.ecplaza.net)

There are two procedures of subsurface resistivity measurement. These may be either sounding survey or profiling survey. The methods vary in the type of target they are looking for and their measurement layout. The electrical sounding survey, also known as Vertical Electrical Sounding (VES), measures vertical variation of the subsurface at a point by assuming homogenous horizontal layer of the Earth, while profiling survey measures the lateral resistivity variation of the subsurface by assuming homogenous vertical variation in electrical properties of the Earth. In this work, Vertical Electrical Sounding (VES) has been used, as it is the most widely and commonly employed technique for groundwater resources potential studies.

3.2.2. Principles of Vertical Electrical Sounding (VES) Survey

In Vertical Electrical Sounding (VES), the positions of the electrodes are changed with respect to a fixed point known as 'sounding point' and the measured values reflect the vertical distribution of resistivity values as a result of the geologic setting. The technique is extensively used in hydrogeological investigation to define horizontal zones of porous strata (Kearey et al., 2002). The basis of the resistivity survey is that, when current is applied by conduction into the ground through a pair of electrodes, any subsurface variation in conductivity alters the current flow within the Earth; this in turn affects the distribution of electric potentials (Everett, 2013).

In spite of the availability of various electrode configurations in electrical resistivity survey, three of the configurations (Wenner, Schlumberger, and the Dipole-Dipole arrays) are the most commonly used (Telford et al., 1990; Kearley et al., 2002). Out of these, the Schlumberger array finds wide application in VES surveys owing to its simple field layout and increased depth of investigation. In this technique, a pair of electrodes used to inject current are systematically increased (while keeping the other two potential measuring electrodes fixed, to some extent) attaining deeper and deeper flow of current and hence investigation depth. In employing this array type, site selection is extremely significant with the Schlumberger array, because it is sensitive to conditions around the closely spaced inner electrodes.

The starting layout of electrodes in a typical Schlumberger array used to collect data in this research work is as shown in (Figure 3.2). This technique was implemented by injecting electrical current (I) into the ground by means of two current electrodes and measuring the resulting potential difference (ΔV) by another pair of potential electrodes placed close to the center of the array. Using the measured values of ΔV, and I, at the measurement point, the resistance of the ground (R) is determined using the Ohm's law as:

$$\Delta V = IR \tag{3.1}$$

The resistance is related with resistivity of the ground with the relation

$$\Delta V = \frac{I\rho_a}{2\pi}\left(\frac{1}{r}\right) \tag{3.2}$$

where, 'r' is the distance from the ground to the first electrode.

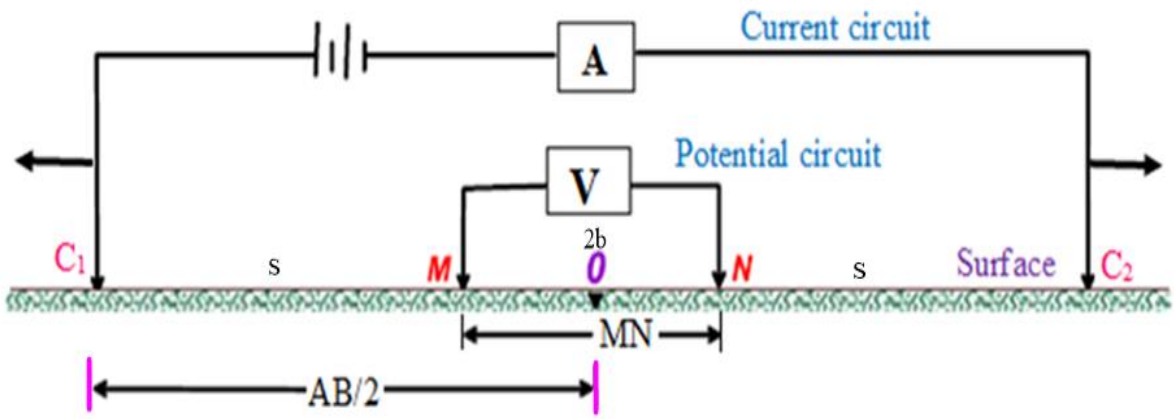

Figure 3. 2 The Schematic plan of the Schlumberger electrode configuration, C_1 and C_2 are the current electrode, and P_1 and P_2 are the potential electrode (Loke, 2004).

When a four electrode system, with two current and two measuring electrodes is employed with distances between them as shown in Figure 3.2, the potential at point M is given by,

$$Vp = \frac{I\rho_a}{2\pi}\left(\frac{1}{r_1} - \frac{1}{r_2}\right) \tag{3.3}$$

and similarly the potential at point N,

$$Vp = \frac{I\rho_a}{2\pi}\left(\frac{1}{r_3} - \frac{1}{r_4}\right) \tag{3.4}$$

The potential difference between points M and N is hence,

$$\Delta V = \frac{I\rho_a}{2\pi}\left(\frac{1}{r_1} - \frac{1}{r_2} - \frac{1}{r_3} + \frac{1}{r_4}\right) \tag{3.5}$$

Consider a subsurface consisting of finite number of layers separated by horizontal boundary planes with the deepest layer extending to infinite depth, the other layers having thickness $h_i = h_1, h_2$.... and each of the layers are electrically homogeneous and isotropic. The field is generated by point source of current located at surface.

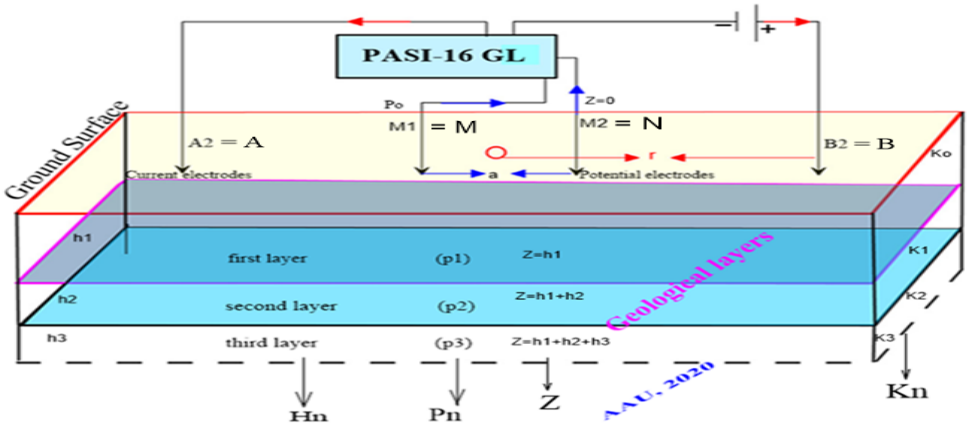

Figure 3. 3 A multi-layer Earth and problem presentation for solution of the potential over a stratified Earth (modified after Loke, 2004).

In the Figure 3.2 the current and potential electrode separations are, r_1= s-b; r_2= s+b; r_3= s+b, and r_4= s-b and therefore, from (3.5)for Schlumberger array,

$$\Delta V = \frac{Ip}{2\pi}\left[\left(\frac{1}{s-b}-\frac{1}{s+b}\right)-\left(\frac{1}{s+b}-\frac{1}{s-b}\right)\right] \tag{3.6}$$

Simplify equation (3.6)given as,

$$\Delta V = \frac{Ip}{2\pi}\left(\frac{2b}{s^2-b^2}\right) \tag{3.7}$$

Therefore, the Schlumberger apparent resistivity can be written as,

$$p_{as} = \pi\left(\frac{s^2-b^2}{2b}\right)\left(\frac{\Delta V}{I}\right) \tag{3.8}$$

3.2.3. Resistivity of Earth Materials

Resistivity of rocks and Earth materials mainly depends up on the water content (porosity), the resistivity of the water/ fluid filling the pores, the clay content and the content of metallic minerals contained (Bernard, 2003). According to Bernard, (2003) expression igneous and metamorphic rocks have high resistivity value. The resistivity of these rocks is dependent on the degree of fracturing and the percentage of the fractures filled with groundwater. Sedimentary rocks, which are usually more porous and have higher water, have lower resistivity values as compared to igneous and metamorphic rocks. To identify the presence of groundwater from resistivity measurements, the absolute value of the ground resistivity must

be considered, because the resistivity of the rocks is largely dependent on the porosity of the rocks and the salinity of the contained water (Bernard, 2003). Table (3.1) gives values of resistivity of some rock materials. These variations in rock resistivity and their measurement are used as diagnostic tool to distinguish between different rock types and whether the rock has pore spaces filled by fluids and the type of fluids (water, gas or oil) filling the pores.

Table 3. 1 Resistivity values for Earth materials (Bernard, 2003)

Earth material	**Normal resistivity (Ohm-m)**
Sandstone	200-5000
Weathered sandstone, moist sandstone	50-200, 56-160
Tuff, welded tuff	30-140, 40-164
Scoria basalt	90-112
Ignimbrite, fractured ignimbrite	100-350, 20-160
Fresh/massive ignimbrite, Highly weathered ignimbrite	213 - 312, 10-120
Top soil	250-1700
Silt clay	5-10
Clay, dry clay	2-20, 20-63
Moist top clay soil	9.4-18
Pumice	10- 85 (wet)/65-220 (dry)
Numerical value for various types of water and saturated rocks	
Groundwater	30-100
Very fresh water	200-220
Salted water	10-20
Sea water	0.3-10
Sea water saturated gravel	0.5-5
Possible fluid saturated ignimbrite	14-56
Water saturated basalt	400-2000
Water in alluvial layer	10-30
Sand contain saturated fresh water	50-500

The three most common characterization of aquifer techniques are: (1) Iso-resistivity (2) Anisotropy and (3) Fracture porosity

The iso-resistivity map showing the resistivity distribution of the aquifer layers has been proven to be useful in mapping promising areas for groundwater abstraction (Ishola et al., 2013).

Basically, the concept of anisotropy (λ) shows the fluctuation of water table in the subsurface of the Earth and which is derived from the parameters transverse resistivity (ρt) and longitudinal resistivity (ρl), where the block of layers as one unit behaves like an anisotropic medium characterized by the longitudinal and transverse resistivities (Maillet, 1947). The coefficient of anisotropy is generally 1 and exceeds 2 in most of the geological conditions (Zohdy et al., 1974).

The fracture porosity values correlate well with the high and low values of anisotropy (λ) suggesting a positive correlation, as can be seen in Figure 5.18. Thus, the calculated porosity value of an aquifer, using an average resistivity, results in an averaged porosity value (Niwas and Celik, 2012).

3.3. Basic Concepts and Principles of the Magnetic Method

A) Magnetic force and magnetic field

The magnetic force as given by Coulomb's law for magnetic poles, symbolically analogues to point masses of gravitational force (Telford et al., 1990). According to their definition, if two magnetic poles of strength p_1 and p_2 are separated by a distance "r", a magnetic force (F_m) exists between them, and is expressed as:

$$F_m = \frac{1}{\mu}\frac{P_1 P_2}{r^2} \tag{3.9}$$

where, 'μ' is constant of proportionality known as the magnetic permeability of the medium.

B) Permeability and susceptibility

Then intensity of magnetization (I) is related to the strength of the magnetic force field (F) through a proportional constant, K and is given by

$$I = KF_m \tag{3.10}$$

where, K is the magnetic susceptibility.

Telford et al., (1990) also defined that the force associated with the magnetic field strength (Fm) is characterized by the magnetic induction (B) as given by

$$B = \mu F_m \tag{3.11}$$

where $\mu=\mu_o \mu_r$ the permeability of the medium and can be defined as the product of relative permeability (μ_r) and permeability of the free space (μ_0).

Thus,equation (3.11) can be written as

$$B = \mu_0 (1 + K) F_m \tag{3.12}$$

By introducing $K= \mu_r -1$ and rearranging we have

$$B = \mu_0 (F_m + I) \tag{3.13}$$

3.3.1. Magnetic properties of rocks and its susceptibility

In geologic interpretation of magnetic data, knowledge of rock magnetic properties for a particular study area requires an understanding of both magnetic susceptibility and remanent magnetization (Slichter, 1929). Those factors influencing rock magnetic properties for various rock types are summarized by (Reynolds et al., 1997). According to Telford et al., (1990) the larger the susceptibility the greater intensity of magnetization and the anomaly produced relative to the Earth's magnetic field will be bigger.

The susceptibility of a rock depends on the magnetite content, so most rocks that have a significant concentration of ferro- and or ferri-magnetic minerals will have the highest susceptibilities. Basic and ultra basic rocks have the highest susceptibility, while igneous and metamorphic rocks have intermediate to low susceptibilities. Sedimentary rocks generally have very small susceptibility (Milsom, 2003). The magnetic susceptibility of common rock and mineral ores is shown in (Table 3.2).

3.3.2. The Earth's Magnetic Field

The observed magnetic field on the Earth's surface can be broken into three separate components (Reynolds, 1997). These three components are: 1) the main field, 2) the external field and 3) the crustal field resulting from variations in lithologic units in the subsurface.

Table 3. 2 Magnetic susceptibility of common rocks and minerals in rationalized SI unit (After Milsom, 2003).

Common rocks	**Magnetic susceptibilities (SI)**	**Ores**	**Magnetic susceptibilities (SI)**
Rhyolite	0.00025-0.01	Hematite	0.0001-0.001
Gabbro	0.001-0.1	Magnetite	0.1-20
Green sandstone	0.0005-0.001	Chromite	0.0075-1.5
Basalt	0.001-0.05	Pyrhotite	0.001-1
Granulite	0.0001-0.05	Pyrite	0.0001- 0.005

The Main Field (secular part): it accounts for over 99% of the Earth's total magnetic field that is caused by convection currents of conducting materials (mainly iron and nickel) within the liquid outer core.

According to Reynolds (1997), the main field consists of several magnetic elements, which are important in determining the measured magnetic anomaly patterns. These include: 1) magnitude of the field (F), 2) magnetic inclination (I) which is the dip of a magnetic compass needle from the horizontal and 3) magnetic declination (D) which is the angle between the geographic and magnetic north's'. Figure 3.3 shows the relationship between these components.

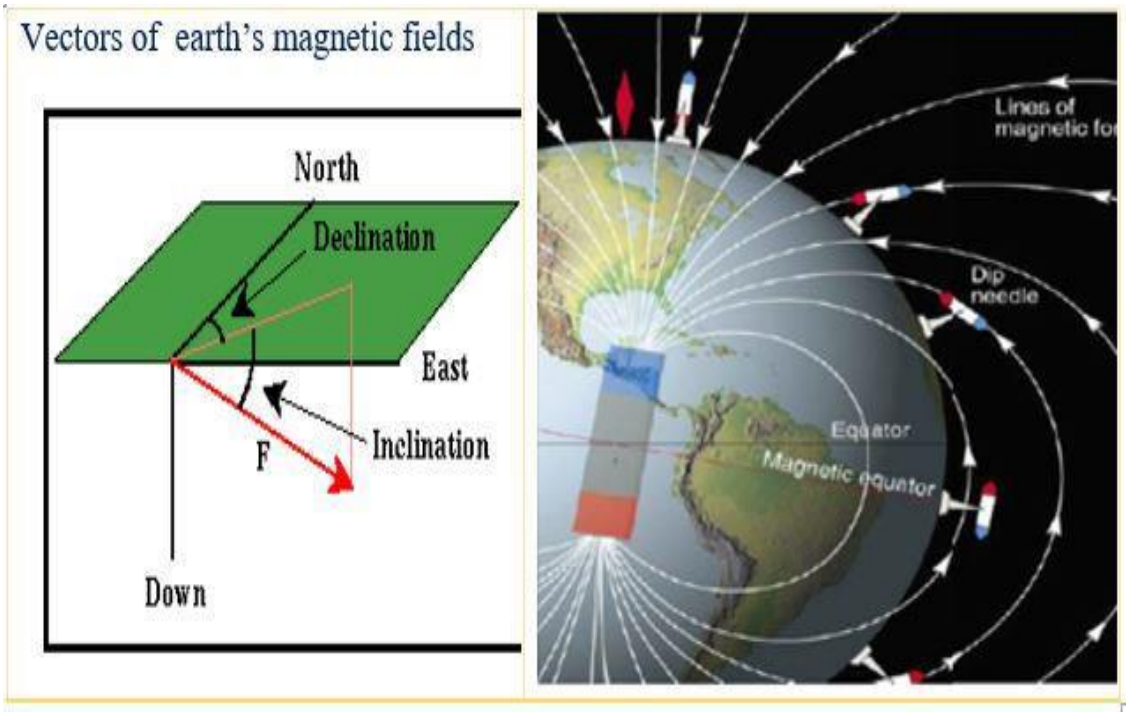

Figure 3. 4 Magnetic elements of the Earth's magnetic field (Image extracted from http://www.geomag.colorado.edu)

The External Magnetic Field (diurnal part): this part of the Earth's magnetic field is due to currents within the Earth's ionosphere. These currents are mainly caused by interactions with plasma connected with solar winds. The time variations of this field portion are much more rapid than that for the main field and are caused by phenomena external to Earth's interior (Telford et al., 1990).

The Crustal (anomalous) Field: this field is the portion of the Earth's magnetic field associated with the magnetism of crustal rocks. The magnetizable materials within the Earth's crust create small amplitude magnetic fields that cause spatial variations of the Earth's measured magnetic field (Reynolds, 1997).Generally, the Earth's total magnetic field can be expressedin a given equation (3.14).

$$B_t = B_{ext} + B_{\text{int}} = B_{ext} + B_D + B_{rm} \qquad (3.14)$$

Where, $B_t$is the total magnetic field, B_{ext} is external magnetic field, B_{int} is the internal magnetic field, B_D is the dipole field which is mainly generated by the fluid outer core, and B_{rm} is the field of rock remnant magnetism.

3.3.3. Magnetic Survey Instruments

Magnetometers do not drift and base readings are taken solely to correct for temporal variation in the measured field (Kearey et al., 2002). Because of the highly variable temporal variations of magnetic field, the Earth's magnetic field cannot be represented by stationary values. Instruments used in geophysical exploration- magnetic survey- can basically be classified in to three groups: i) the torsion (and balance), ii) fluxgate and iii) resonance type magnetometers. Magnetometers measure horizontal and/or vertical components of the Earth's magnetic field or the total field.

Magnetic balances: The oldest version of this instrument is obtained by the torque of the Earth's magnetic field balances with the gravity effect at the centre of gravity. The angle of pivot is a function of the magnetic field, and is measured by a light beam that is projected onto a scale.

Flux-gate magnetometers: The construction of this rather expensive but highly sensitive instrument involves two coils wound in opposition. A current is passed through one to induce magnetization. In the absence of the Earth's field, the fields of these two cancel out. An alternative current (AC) is applied that saturates the cores in opposition in the absence of the Earth's field. The Earth's field reinforces one core and opposes the other.

Proton precession magnetometer: The most commonly used magnetometer for both field survey work and observatory monitoring is currently the proton precession magnetometer. The sensing device of the proton magnetometer is a container filled with a liquid, rich in hydrogen atoms, such as kerosene or water, surrounded by a coil (Kearey et al., 2002). Field instruments working on this principle provide absolute readings of the total magnetic field.

In this thesis work, the Proton precession magnetometer (GSM- 19T) has been used, so as it is the most widely and commonly employed technique to delineating the lithologic unit of the subsurface, which control the flow and movement of groundwater in the survey area.

3.3.4. Data correction for magnetic variations

To remove all causes of magnetic variation from the observations other than those arising from subsurface geology it is necessary to make correction of magnetic data. In ground magnetometer surveys, it is always appropriate to keep the sensor away from obviously

magnetic objects such as cars, power lines, metal pipes, electrified railway lines, etc. Common corrections in the processing of magnetic data includes; diurnal correction, leveling, IGRF, gridding, and reduce to pole accordingly, the two most relevant correction of magnetic variations encounter in this research work.

Diurnal correction: The most significant correction is for the diurnal variation in the Earth's magnetic field. The necessary corrections are mostly attempted by the reoccupation of the base station, which is located in or near the survey area. On land, the magnetometer is read at a fixed base station periodically throughout the day. The magnetic data were corrected for diurnal variation and removal of unwanted/noise readings though close examination of the data. The simple formula to execute this operation is defined by (eq. 3.15)

$$DC = \left(\frac{BS_2 - BS_1}{T_2 - T_1} \right) (T_r - T_1) \tag{3.15}$$

where: -DC is the Diurnal Correction; T_1 is the Observed time of Base Station-1; BS_1 is the Reading of Base Station-1; T_2 is the Observed time of Base Station-2; BS_2 is the Reading of Base Station-2 and T_r is Observed time of each measuring point.

Geomagnetic correction: International Geomagnetic Reference Field (IGRF) has been prepared from comparison of individual magnetic responses in different areas of magnetic observatories.IGRF determined values of (IGRF, 2010) were used to reduce the resulting data to the magnetic anomalies. Therefore, it has become standard processing practice for magnetic survey that the applicable IGRF (updated to the time of the survey) is subtracted from the observed values of the total magnetic intensity and can be defined as in a given equation (3.16).

$$IGRFC = DC - IGRF \tag{3.16}$$

where, IGRFC is the International Geomagnetic Reference Field Correction.

In order to produce a magnetic anomaly, the data have to be corrected to take into account the effect of latitude and, to some extent, longitude (Reynolds, 1997). The magnetic field produced by the regional susceptibility model is then used as regional field and the residual data are obtained by simple subtraction form the regional anomaly. The advantage of this method of separation are that it introduces little distortion to shape of the extracted anomaly

and that it is not affected significantly by factors such as topography and the overlap of power spectra of regional and residual field. The intention used magnetic surveys in this thesis can be successfully utilized to accurately demarcate the location of fault/ fracture, which governs the flow and movement of groundwater in the area.

CHAPTER FOUR

DATA ACQUISITION, PROCESSING AND PRESENTATION

4.1. General

This thesis work has utilized the survey that consist of the electrical resistivity and magnetic geophysical techniques in order to address the main objectives of the research. The layout of the geophysical survey profile lines and observation points are as shown in Figure 4.1.

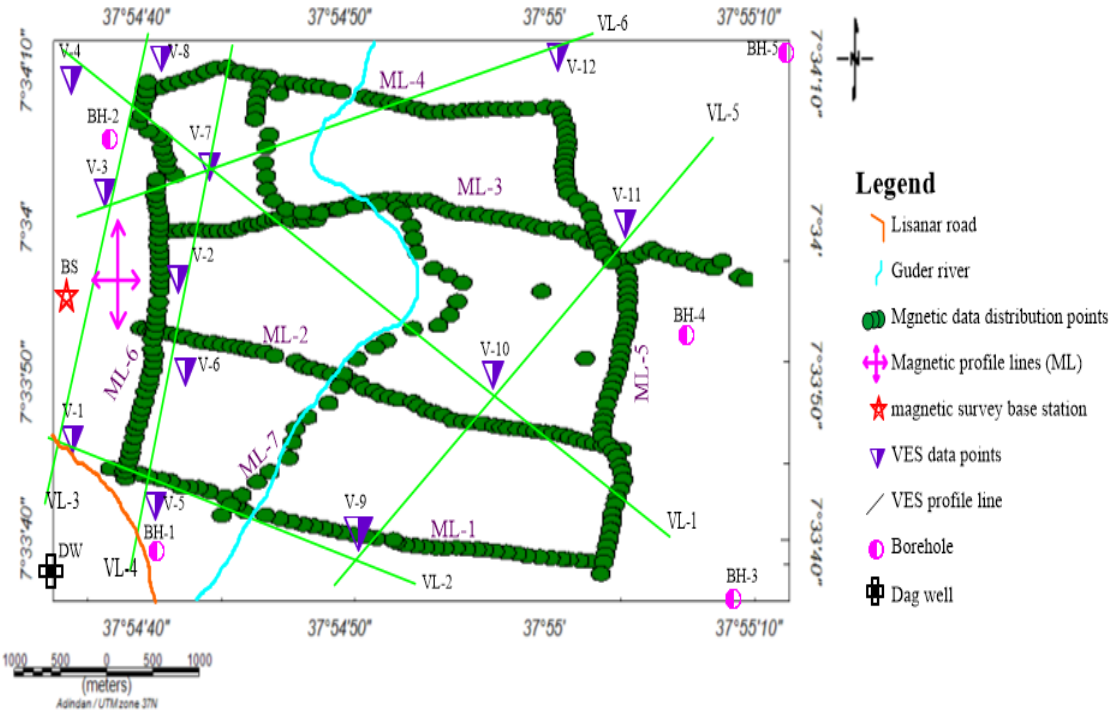

Figure 4. 1 Distribution of VES points, magnetic profile lines and location of boreholes over the study area.

It is clear from Figure 4.1 that the geophysical surveys have been conducted over both sides of Guder River and following its course so that good data coverage and density has been attained with the survey. The number of boreholes available in close proximity to the surveyed area is also an added input to facilitate the calibration of the electrical data and constrain the interpretation. The magnetic data volume and coverage is also believed to be adequate to conduct both contoured mapping and analysis as well as profile plot and 2D modeling of the data.

4.2. Data Acquisition and Field Lines for Electrical Resistivity Survey

The electrical resistivity survey was carried out employing the Vertical Electrical Sounding (VES) technique. A total of twelve sounding points (VES points) were surveyed in the study area along six survey lines, using Schlumberger configuration with max half current electrode spacing (AB/2) max of 500m. The survey lines were oriented in NW-SE and NE-SW directions following the Guder River course and placed on either side of it.

The instrument employed for the Vertical Electrical Sounding (VES) survey is the PSI-16 GL Earth resistivity unit along with the P-100 Energizer (http://pasisrl.en.ecplaza.net) as shown in the (Figure 4.2). Stainless steel electrodes and long cables on reels were used along with meter tape and hammers. Handheld GPS was used to record the sounding point coordinate.

a

b

Figure 4. 2 Photo a) instrument field setup, and b) data acquisition scheme for the Vertical Electrical Sounding survey.

4.3. Processing and Reduction of Electrical Resistivity Survey Data

During field survey, during each sounding, the sounding curve, which is a log-log graph of apparent resistivity versus half the current electrode separations, was plotted, right in the field as a measure quality control.

Data were then processed using RESIXIP and Win RESIST software programs in order to determine the layer parameters (resistivity and thickness/depth) beneath each VES. During data processing using the RESIXIP and Win RESIST software, iterations were continued until best fitting was attained between the field acquire and calculated/theoretical curves. The calculated and the measured resistivity values were adjusted to reduce the error to as much as possible to achievable the minimum value. The apparent resistivity values of each of the VES sites were recorded simultaneously. Overall, error values of 1.9 - 4.7% were achieved showing good data quality.

4.4. Presentation of Electrical Resistivity Survey

The electrical resistivity survey results are presented in the form of VES curves, pseudodepth sections, geoelectric sections, slice-stacked sections Isoresistivity and fractured-porosity. During interpretation of the sounding curves, a 3 to 5 layer subsurface is seen too well represent the subsurface condition of the study area.

Current electrode separation was progressively increased in series of measurements in order to acquire data from deeper horizons. The maximum current electrode separation, (AB/2) = 500m, was chosen based on the anticipated depth to the water bearing horizon and subsurface geology. Larger separation of electrodes was also not possible due to the rough terrain of the area of study. Some of the VES were surveyed near previously drilled borehole to obtain control during interpretation.

At AB/2=20m, 30m, 150m and 220m repeat readings were taken at two different potential electrode positions (MN/2) in order to examine the data quality and also assess any possible effect of anisotropic character of the underlying formations.

In order to ensure consistent and reliable readings, measured results were plotted in the field during the measurement and inconsistent values were repeated to make convinced uniformity in the readings. If any error is detected during data acquisition, it was automatically corrected either by taking repeated measurements or by securing better galvanic contact with the ground through changing the position of the current injection and/or measuring electrodes. The ground condition was fair enough not to require the use of saline water or otherwise. The location of the sounding points is as given in Table 4.1.

Table 4. 1 Location of sounding (VES) points in UTM coordinates.

VES No	UTM Coordinates (m)			Remark
	Easting (E)	Northing (N)	Elevation (M)	
1	380081	836504	2167	On line – 2 & 6
2	380202	836806	2169	On line - 3
3	380159	836995	2177	On line – 2 & 5
4	380124	837274	2174	On line - 1
5	380166	836437	2149	On line – 3 & 6
6	380203	836639	2151	On line - 3
7	380267	837021	2161	On line – 1 & 5
8	380205	837311	2173	On line - 2
9	380296	836431	2151	On line – 4 & 6
10	380459	836591	2166	On line - 4
11	380754	836772	2178	On line - 4
12	380692	837215	2172	On line - 5

4.5. Data Acquisition and Distribution of Magnetic Survey

The observations were made every 10m over all transect lines of the VES and at 20m station spacing for each random field distribution points. All the magnetic data were collected over two days with the survey designed to commence during the morning hours with a view to reducing the diurnal effects on the data., However, survey were also taken in the late afternoon hours to optimize the field time available for the survey. For this study, the base station was reoccupied within one and half hour interval to facilitate correction of diurnal variation.

A typical set up for the magnetic survey using GSM- 19T (http://www.gemsys.com), Proton Precision Magnetometer is illustrated in (Figure 4.4) were one person carries the sensor on stadia while the other holds the measuring instrument, taking the total field as well as location readings and repeat readings as may be required. Data are checked for consistency and if variations more than a few nT are seen in repeat measurements, readings are taken repeatedly and in such instances average values of readings are recorded.

Figure 4. 3 Magnetic data acquisition using the proton precession magnetometer (GSM-19T).

4.6. Data Processing and Reduction of Magnetic Survey

At the beginning, for establishing the base station the first thing that was done to look for appropriate location of a point close to the survey area with less magnetic noises such as Cars/ Vehicles, Power lines, Metal sheet houses and others. The measuring personnel establish magnetically free environment by removing magnetic material like belts, watches, mobile phones and any objects made of metallic material. Data acquisition was always started and ended at the base station. As mentioned earlier, repeat measurements were taken at regular intervals to effect correction for diurnal variation. The processing of the magnetic data revealed a set of processes such as diurnal correction and IGRF correction. Diurnal correction was done by subtracting the diurnal variation of each reading point.

4.7. Presentation of Magnetic Survey Data

The positions of the survey stations and the station elevations were determined using the GPS receiver. This magnetic survey has specifically one base station, which located at a UTM coordinate of 380129 Easting and 836873 Northing. The survey lines where oriented in the general direction of east west, northwest and southeast so as to detect the presence of possible structures that could control groundwater occurrence, accumulation and flow

patterns. Magnetic survey involves measurement of the sum of magnetic field produced by local and regional magnetic fields.

Magnetic data analysis in this thesis work involves:

i) Removal of unwanted and spurious erroneous magnetic data through visual inspection,

ii) Making the corrections using the base station readings for the respective closed loops,

iii) Removal of the main field of the base station readings; this is done by using two procedures a) using the IGRF value for the base station and/or b) using the averaged value of all readings taken at the base station,

iv) Determine and plotting the magnetic anomaly,

v) Regional-residual separation and producing the respective regional and residual maps,

vi) Euler Deconvolution plots for depth to causative body/source mapping,

vii) 2D modeling of the data for selected profile producing a number of upward continued/derivative maps

CHAPTER FIVE

INTERPRETATIONS, RESULTS AND DISCUSSIONS

5.1. General

In this thesis work, interpretations have been done based on the combination of results from vertical electrical sounding and magnetic data with the help of a borehole lithological log data to constrain the results. In the following sections interpretation of the electrical resistivity and magnetic data is done. For the electrical data, the apparent resistivity data and the interpreted layer parameters of each sounding curve were used to produce different sections, which show contrast in the resistivity and depth of the subsurface rocks. As the final result of the electrical survey interpretation, the geoelectric sections are the results of interpreted true resistivity parameters of the subsurface and are believed to represent the subsurface electrical stratification more practically. On the other hand, from magnetic data residual anomaly plots, magnetic profile plots and 2D model sections that, show subsurface lithology variation and existence of possible structures over the surveyed area, were prepared and presented.

5.2. Interpreted VES Curves

A combination of software has been used for the purpose: RESIXIP and Win Resist software's (Velpen, 1995) for interpretation of the individual VES data. During interpretation of theVES curves, a very good correlation between the field data and interpreted model parameters are obtained for all the VES points. As an illustration, the interpretation of sounding data of VES-1, VES-2and the possible lithologic interpretation of result of VES-3 constrained with data from the BH-2,(named asTachegnaw Gode)are shown in Figure 5.1. Interpreted VES curvesfor the rest of the soundings and the lithologic logs of six borehole descriptions are found at Appendix-1and -2 respectively. It is seen as well that, RMS errors of 2.7, 2.4 and 1.9 are obtained for VES-1, -2 and -3 correspondingly, showing good fit between the field data and the models and also an indication of good quality field data.

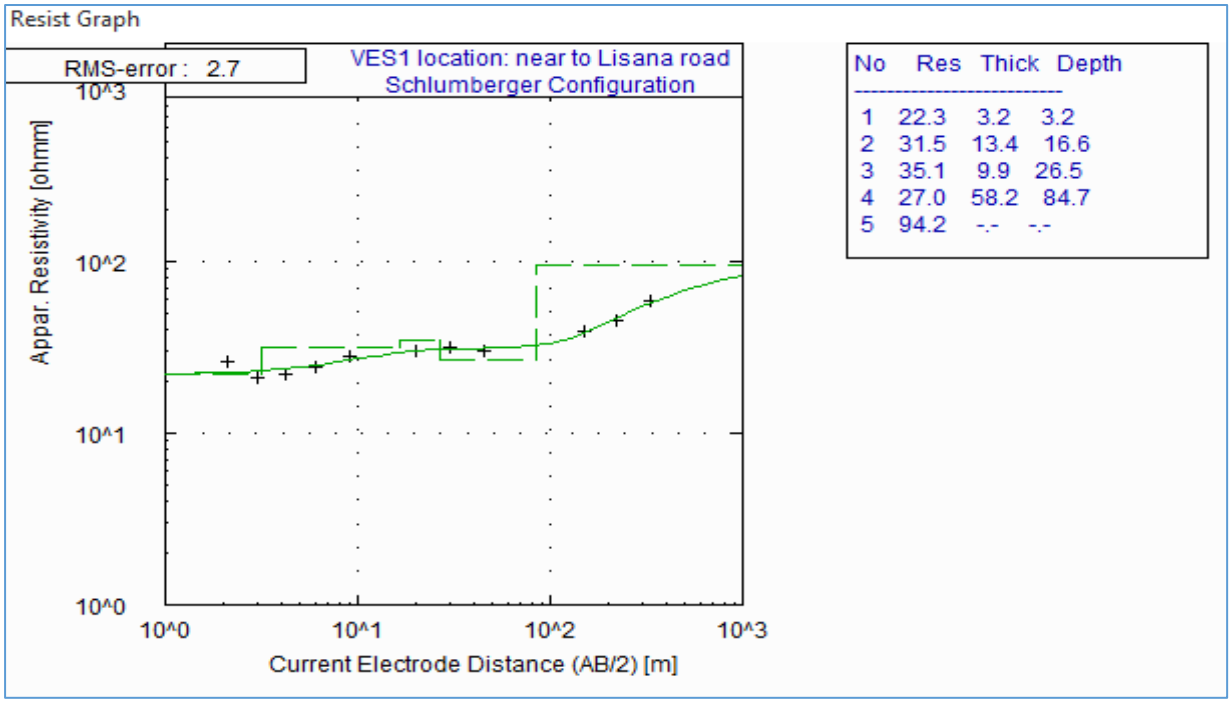
Resist Graph
RMS-error : 2.7
VES1 location: near to Lisana road
Schlumberger Configuration
Appar. Resistivity [ohmm]
10^3
10^2
10^1
10^0
10^0
10^1
10^2
10^3
Current Electrode Distance (AB/2) [m]
No Res Thick Depth
1 22.3 3.2 3.2
2 31.5 13.4 16.6
3 35.1 9.9 26.5
4 27.0 58.2 84.7
5 94.2 -.- -.-

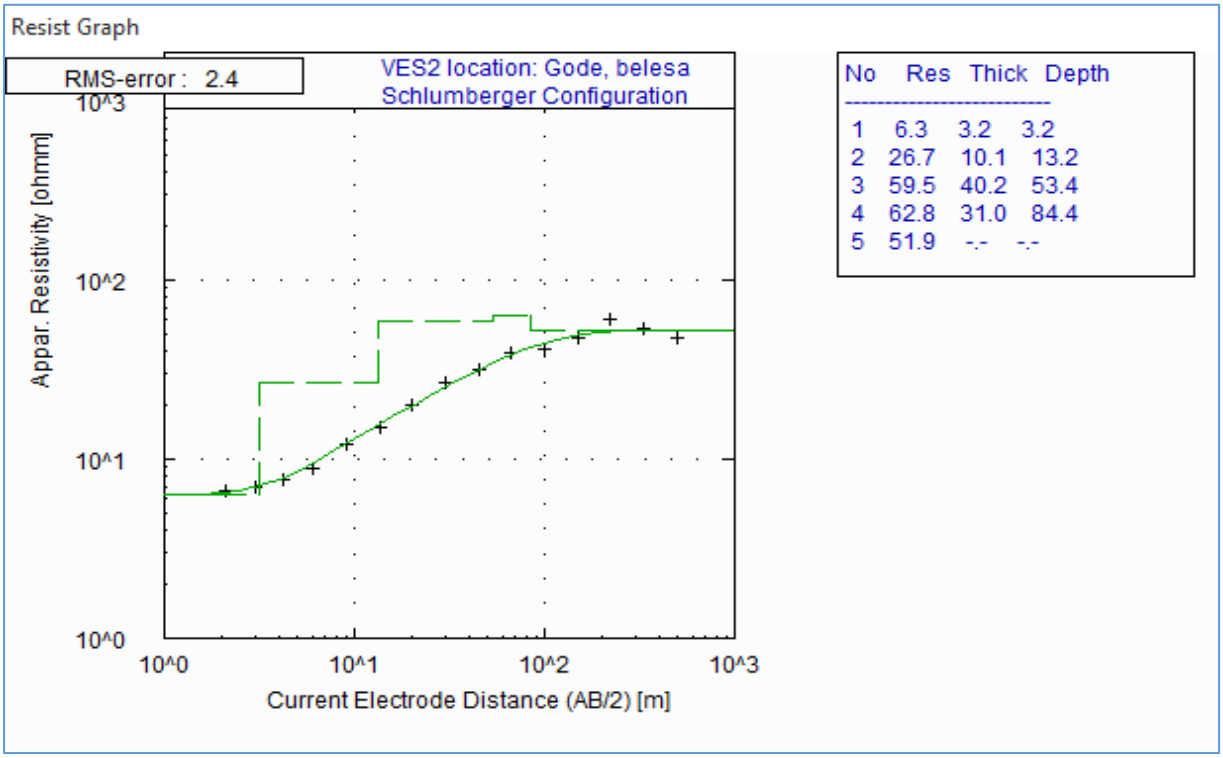
Resist Graph
RMS-error : 2.4
VES2 location: Gode, belesa
Schlumberger Configuration
Appar. Resistivity [ohmm]
10^3
10^2
10^1
10^0
10^0
10^1
10^2
10^3
Current Electrode Distance (AB/2) [m]
No Res Thick Depth
1 6.3 3.2 3.2
2 26.7 10.1 13.2
3 59.5 40.2 53.4
4 62.8 31.0 84.4
5 51.9 -.- -.-

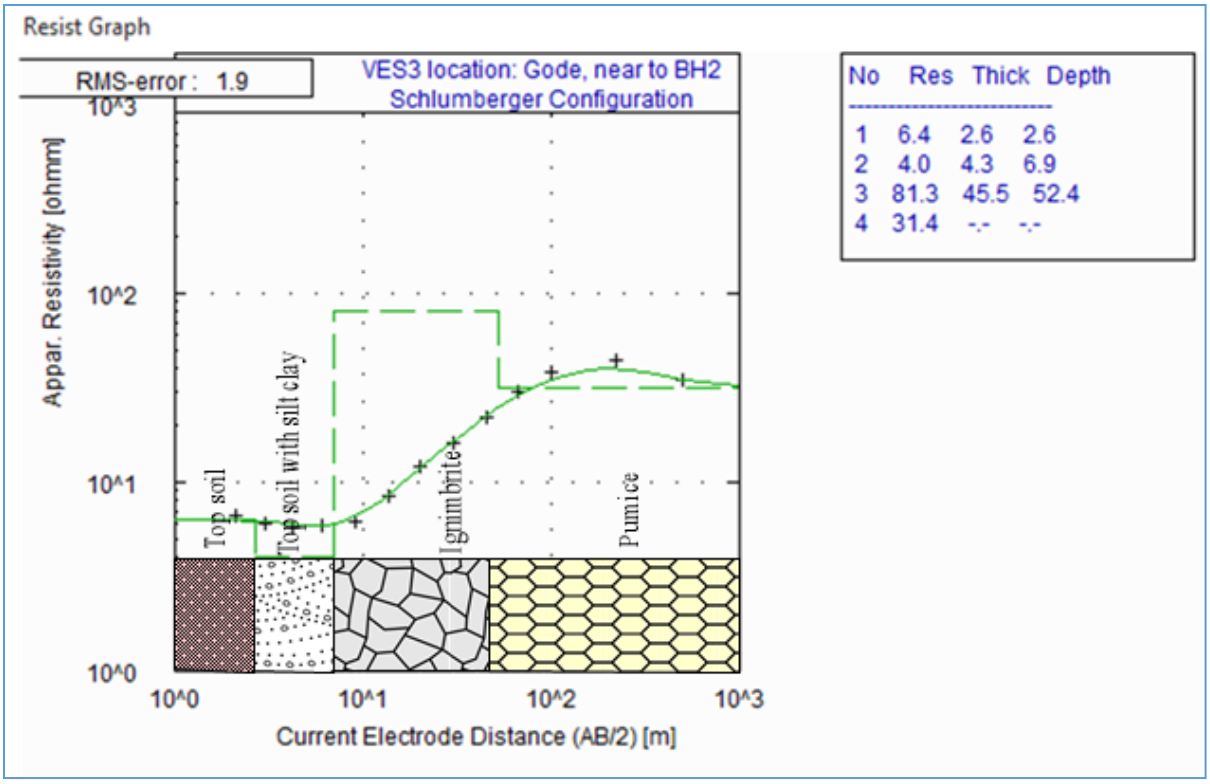

Figure 5. 1 Examples of interpreted VES curves of three sounding pointsVES-1, -2 and -3, showing good correlation between the field data and the fitting model.

5.3. Pseudodepth and Geoelectric Sections for the Different Survey Profiles and their Interpretation

Pseudodepth section is an essential method of presenting the measured apparent resistivity values. The raw field data collected for each sounding is gridded and displayed as regular contour map, as a result, areas of high or low anomalous resistivity values are easily observed shown from the plots. The pseudodepth sections have been generated from the VES for selected profiles where the VES points appear in line by using Surfer v.16 software (http://www.goldensoftware.com). On the other hand, the most useful and final form of presentation of resistivity sounding data is the geoelectric section. This is achieved by interpreting the individual VES in terms of true resistivity and thickness of the subsurface layers and joining the results of the VES for those points that lie on a line. Layers with small thickness are not quite apparent on the geoelectric section due to a scale factor. Lithologic logs of more than five boreholes and one dug well that are exist near the survey lines were used to fix the thickness of each subsurface layer during the VES interpretation. It is not

possible to constrain the depth of each geoelectric layer all over the survey line on the basis of borehole logs, rather, it is possible to derive trial-and-error models that match the VES data sets, coincident with borehole data. The software employed to construct the section is Auto Cad (2010), (http://www.knowledge.autodesk.com).

In the following sections, the pseudodepth and geoelectric sections for six selected profile lines (Figure 4.1) are constructed and discussed separately.

5.3.1. Pseudo Depth Section for Line-1

The pseudo depth section assembled from apparent resistivity data of VES- 4, 7 and 10 that lie on survey Line-1 oriented in a northwest direction and crossing Guder River at its southeast end (Figure 4.1) is given in Figure 5.2. The projection line runs in NW-SE direction. According to this plot, there is a distinct lateral variation in resistivity showing low resistivity at the top layer of VES-4 and VES-10 is mapped. The high resistivity zone is found only in the region beneath VES-7 whereas; the vast region beneath VES-7 shows extensive coverage of moderate resistivity zone. In the region between VES-4 and VES-7, the subsurface is represented by relatively conductive horizon, and this to some extent is also the case beneath VES-10 showing low resistivity region, which are indicative of potential water saturation in the southeastern part of the map (Figure 5.2). Here, between VES- 4 and VES7 the existing resistivity variation possibly shows the existence of contact shown by dashed solid line.

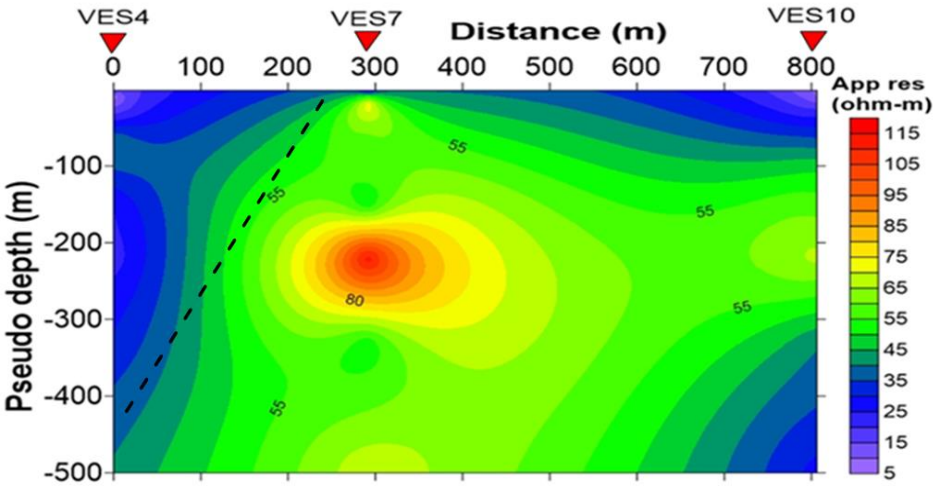

Figure 5. 2 Apparent resistivity pseudodepth section along Line-1.

5.3.2. Geoelectric Section for Line-1

Figure 5.3 represents the geoelectric section constructed using the interpreted layer parameters of sounding data from VES- 4, VES- 7 and VES- 10, in addition the lithology log from nearby borehole-2. The lithological description of the borehole depth section used for modeling is given in Appendex-2. Three geoelectric layers represent the subsurface beneath the projected line (see Figure 5.3). A very thin top soil with varying resistivity response is due to the changing moisture content is mapped as the first layer along the line. The second broad horizon of the geoelectric layer corresponds to moderately saturated ignimbrite layer. The layer may represent highly weathered, possibly water saturated ignimbrite. The high resistivity (165Ω-m) response of the third layer beneath on VES- 10 may be attributed to dry pumice with sand, presumably devoid of water. This is underlain by a high resistivity layer with thickness varies from 57m bellow VES- 7 to 83m near VES- 10, but with increasing the depth the resistivity gradually decreased this could be the presence of moist pumice underneath on VES- 10. The weak zone, which represented solid dash line, is existed between VES-4 and VES- 7 shown in Figure 5.3. The last portion, the fourth layer of the geoelectric section shows the low resistivity with the response of highly weathered/ fractured pumice/ volcanic ash, which is possibly water saturated zone found in all part of VES-4, VES-7 and VES-10.

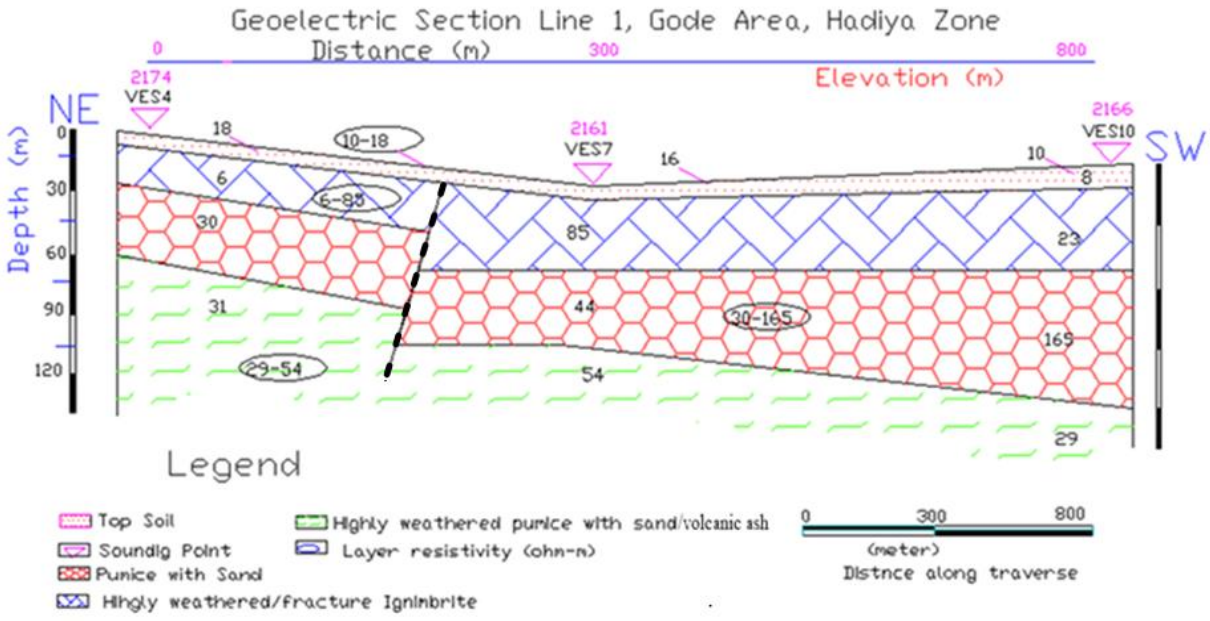

Figure 5. 3 Geoelectric section constructed for Line-1.

5.3.3. Pseudodepth Section of Line-2

The pseudodepth section constructed using VES-1, -5 and -9 that lie on profile Line-2, is given in Figure 5.4. The survey line runs in NW-SE direction (Figure 4.1). The top and bottom substratum is manifested by relatively low resistivity (possiblysaturated) zone and this is mapped beneath VES-1 and this low resistivity zone extends to the middle portion of VES-5 and VES- 9. Very high resistivities ranging between 210-325 Ω-m are observed at the top of VES-5 and VES- 9, geologically interpreted as the response of scoracousbasalt/ massive ignimbrite. A nearby BH- 1, named as Misrak Anlemo, which is found at depth of 143m in a given annex-2 is used to interpret the data for the region between VES- 5 and VES- 9. The high resistivity ranging from (110-135 Ω-m) lays between VES- 5 and VES- 9, which shows most probably a horizon devoid of moisture content of rocks underneath the region as shown in (Figure 5.4).

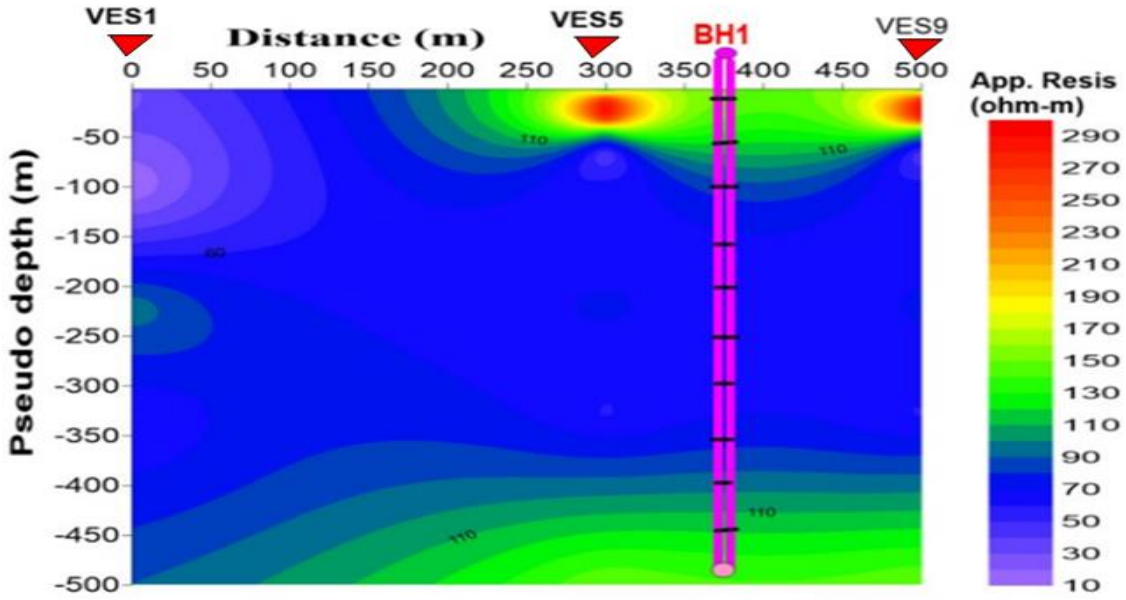

Figure 5. 4 Apparent resistivity pseudodepth section for Line-2

5.3.4. Geoelectric Section of Line-2.

According to Figure 5.5, three to four distinct geoelectric layers represent the subsurface, beneath the surveyed line. The northwest part of the first layer is covered by clay content of top soil, which has a resistivity value of 22 Ω-m. According to the lithology log the second layer from the nearby borehole-1 that is found between VES-5 and VES-9 the resistivity

response, of this horizon corresponds to undifferentiated sequence ofscoracous basalt with pumice/ignimbrite with sand. In essence, the lithological description of the borehole depth section (given in Annex 2) with their resistivity parameters from each interpreted VES were used to prepare the geoelectric section shown below (Figure 5.5). The third broad horizon of the geoelectric layer that corresponds to the moderately saturated ignimbrite with resistivity values varying from 35-58 Ω-m. The layer mapped as the fourth layer on the section is an extensive horizon covering the whole line with resistivity ranges between (74-102 Ω-m). From surveyobjective point of view, the regions on the southwestern side of the end layer (i.e. between VES-5 and VES-9) are zones that a (BH- 1), so called(Misrak Anlemo) sunk to depths in excess of 143m will likely welded pumice with unsaturated horizon is also presented on the nearby borehole-1 at this depth range presumably devoid of water.

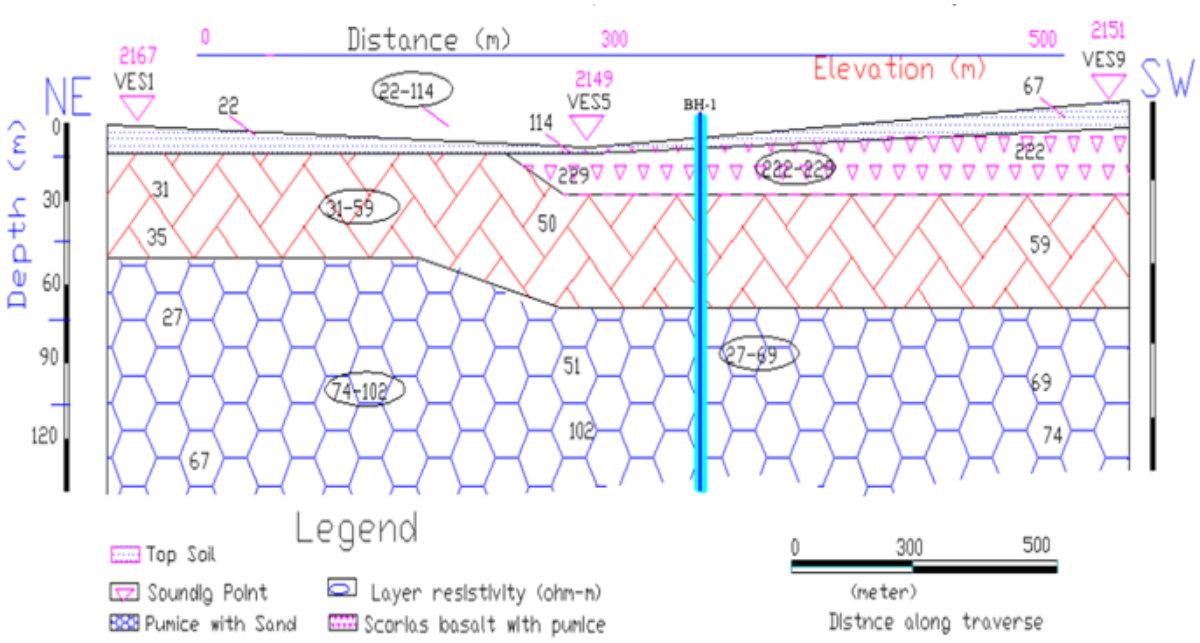

Figure 5. 5 Geoelectric section constructed from interpreted VES on Line-2.

5.3.5. Pseudodepth Section for Line-3

The pseudodepth section for this profile is constructed from three VES points that lie on survey Line-3, i.e. VES-1, -3 and -8, a profile which is oriented in a south to north direction west of Guder River (Figure 4.1) is given in Figure 5.6. According to this figure, most of the top part of the section shows low resistivity zones mapped around VES- 1, VES- 3 and VES-8. This low resistivity zone is also found to extend to some extent in the region around VES-3 and extend to large depth in the region of VES- 8.

Relatively high resistivity responses are found at the middle and bottom region/ portion of VES- 3 and VES- 1 respectively, with the high resistivity values more extensive around VES-1. The region beneath VES-8 is of interest from the point of view of this survey as the low resistivity values are recorded as a result of likely groundwater saturation. A possible structure/contact zone/ is depicted between VES-8 and VES-3 and is shown by the dashed solid line in the (Figure 5.6 and 5.7).

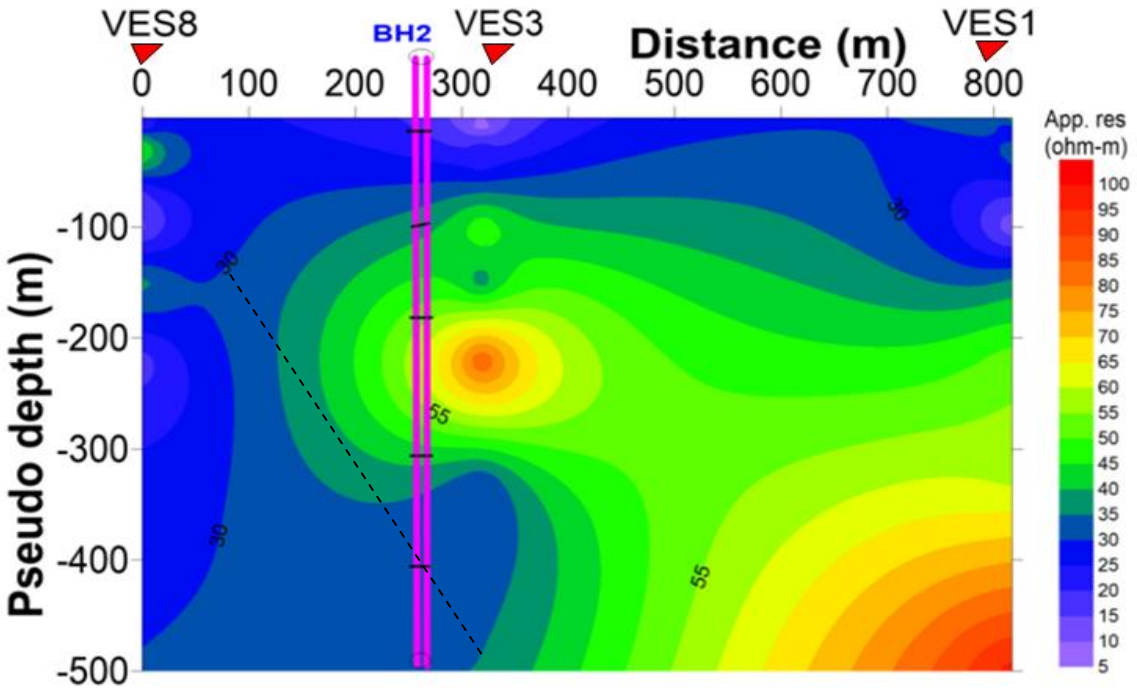

Figure 5. 6 Apparent resistivity pseudodepth section for VES on Line-3.

5.3.6. Geoelectric Section of Line-3.

The geoelectric section along profile line-3 is constructed from the interpreted layer parameters of VES-8, VES-3 and VES-1. From the section given in Figure 5.7, it is seen that the subsurface consists of three geoelectric horizons. The first layer of the geoelectric section thickens from 8m at VES-5 to 20m at VES-5. The formation of second layer resistivity ranging from 32-81Ω-m interpreted as highly weathered and fractured ignimbrite. The northeast part of third layer in the sequence is characterized by relatively low resistivity values varying between 14-31Ω-m. This saturated horizon is also presented on the nearby BH- 2, namely Tachegnaw Gode at a depth below 171m, which interpreted as saturated pumice with sand/ volcanic ash extends to the last portion, presumably flush of water.

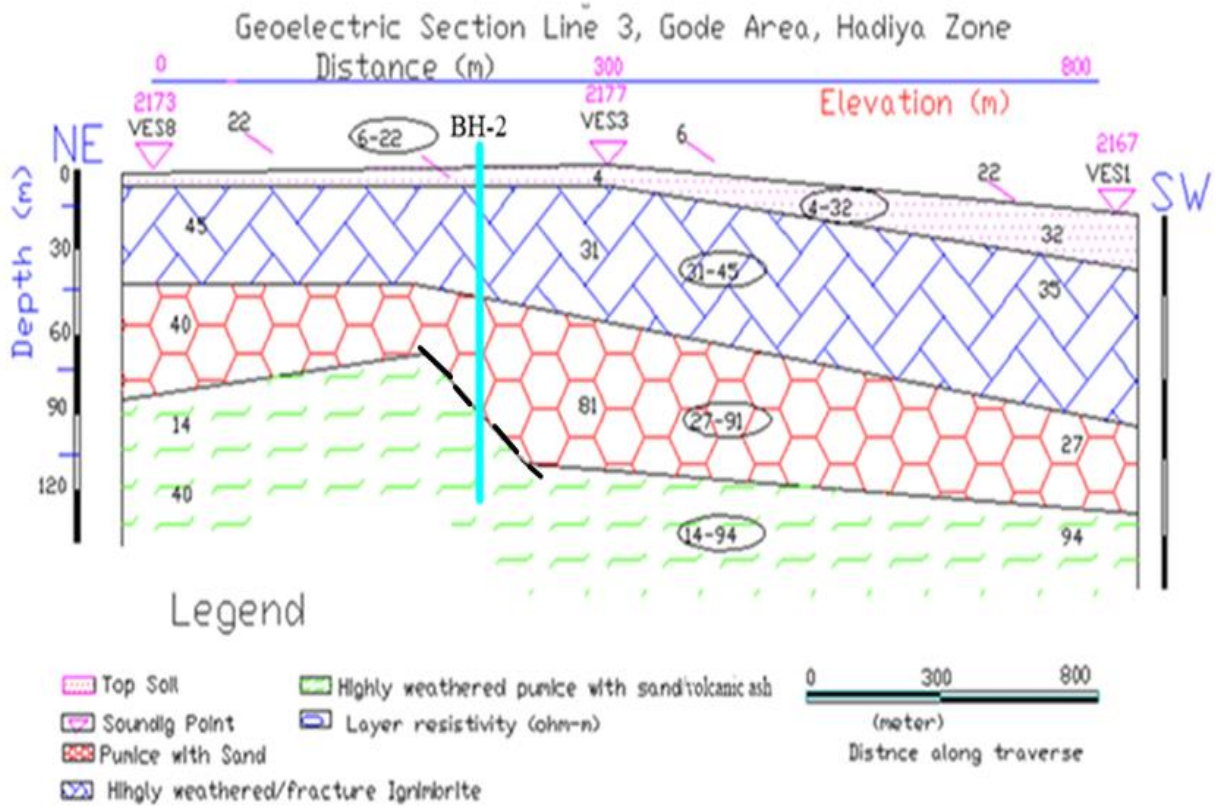

Figure 5. 7 Geoelectric section for survey Line-3.

5.3.7. Pseudodepth Section for Line-4

The apparent resistivity pseudodepth section for Line-4, constructed by using VES- 5, -6 -2 and -7 that is a line running in the SW-NE direction and parallel to Line-3 (Figure 4.1), is shown in Figure 5.8. According to the section, there is a lateral variation in resistivity in the upper most part of the section with prominent high resistivity top regions mapped beneath VES- 5, VES- 6. This relatively high resistivity (180-340Ω-m) zones are not extend to greater depth. The upper layer of VES- 7 shows the low resistivity, whereas, the rest of the section shows extensive coverage of the high resistivity horizon. However, the upper to bottom layer of VES- 2 showlow resistive area, which extends to the middle portion of VES- 5and VES- 6. In the other word, the relatively low resistivity region (40-80Ω-m) which covers the vast region of the section potential water saturated horizon underneath VES-5, VES-6 and all portionVES-2. A probable structure /week zone/ is depicted between VES- 2 and VES-7, which existed at VES- 6 and is shown by the dashed solid line.

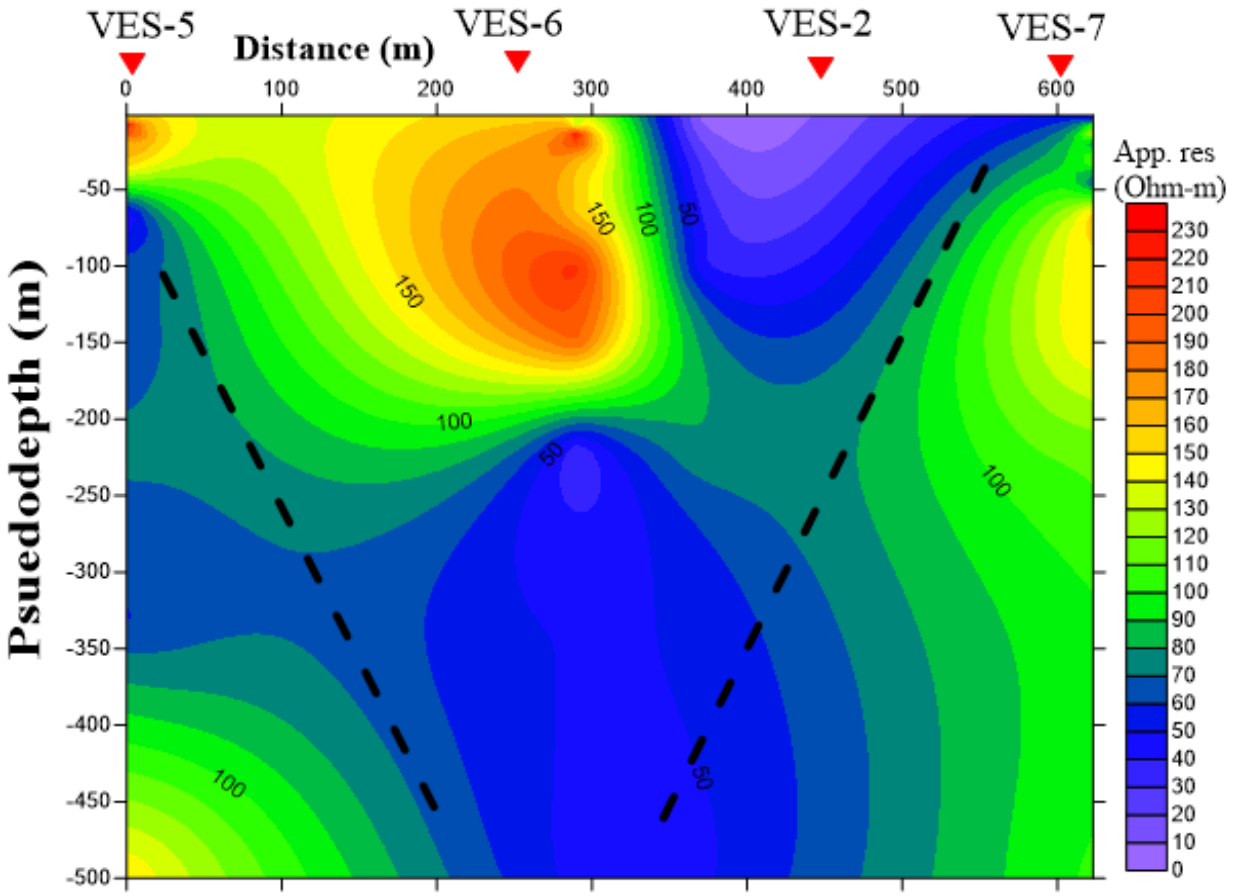

Figure 5. 8 Apparent resistivity pseudodepth section for Line-4.

5.3.8. Geoelectric Section of Line-4.

The resulting geoelectric section constructed from the interpreted layer parameters of VES-5, VES-6 VES-2 and VES- 7 lying on this profile line is given in Figure 5.9. Three to five distinct geoelectric layers represent the subsurface, beneath the projected line. The formation of high resistivity 154-441 Ω-m existed in the northeast part of the second layer interpreted as scoria basalt with pumice (correlate with the lithologic log of BH-2, namely Tachegnaw Gode). The second layer on the section is an extensive horizon of high resistivity covering from the southwestern most end part of the line to southeast direction, with resistivity ranges 51-63 Ω-m. According to Figure (5.9), between VES-2 and VES-6, and between VE-5 and VES-6 inferred geological structure is shown by broken line. This broken line found in the northeast and southwest part of the section attributes the existence of contacts and or weak zone (fractures/ Faults). The low resistivity values again suggest that the layer is potentially water bearing under the last portion of the section.

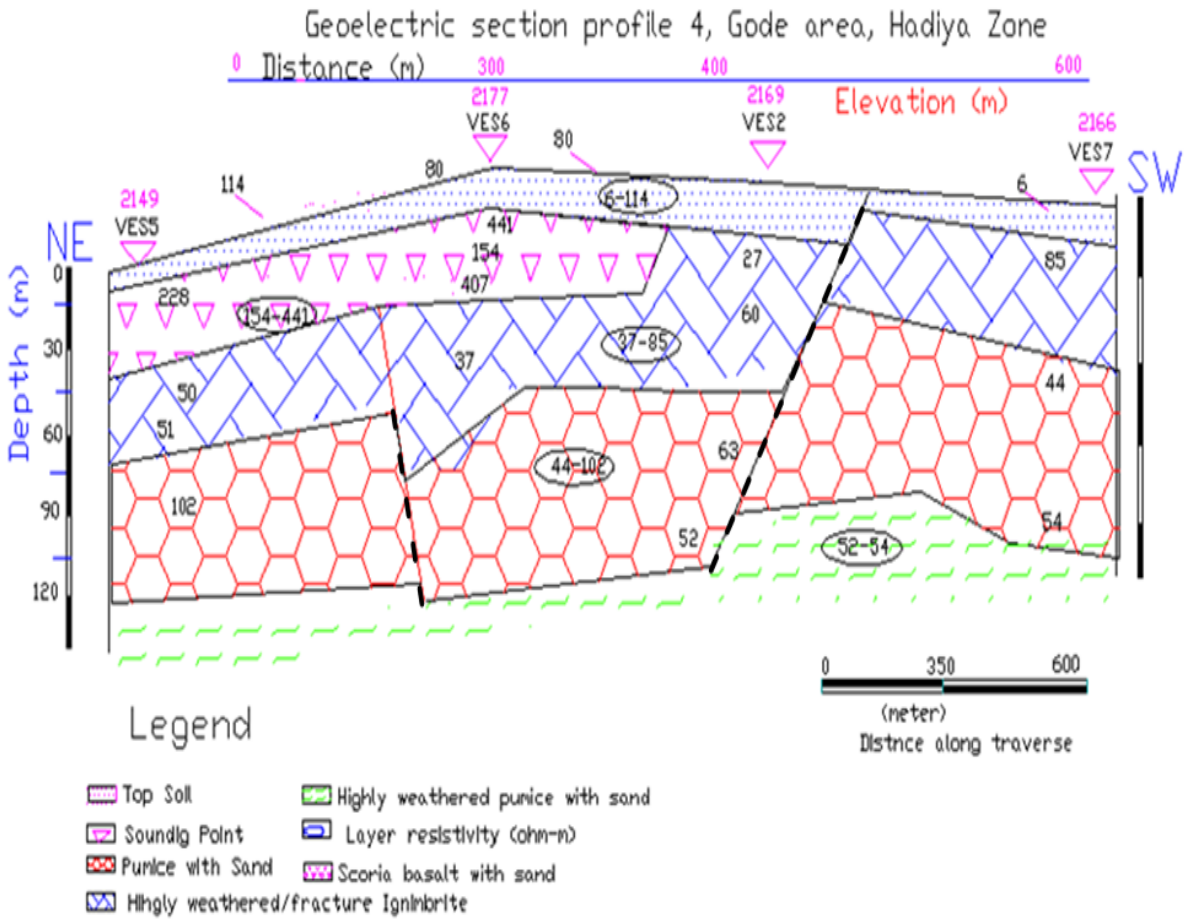

Figure 5. 9 Geoelectric section of survey Line-4.

5.3.9. Pseudodepth Section of Line-5

The pseudodepth section generated from the apparent resistivity data of VES- 9, 10 and 11 is given in Figure 5.10. The projected line runs over in NW-SE direction of the study area. From top, down to the end, the ground section beneath VES- 9 and the middle portion underneath VES-11 are covered by a relatively high resistivity region. Towards the NW along this projected line between VES- 10 and -11, the shallow portion of the ground segment appears to be low resistive and exhibit a gradual increase in resistivity with depth.

Below the middle portion layer of VES- 10 and VES- 11, the low resistivity horizon is mapped. The vast region under the section shows extensive coverage of the low resistivity zone between VES- 10 and VES- 11. These sections can reveal good idea about geologic and hydrogeologic situations of the area.

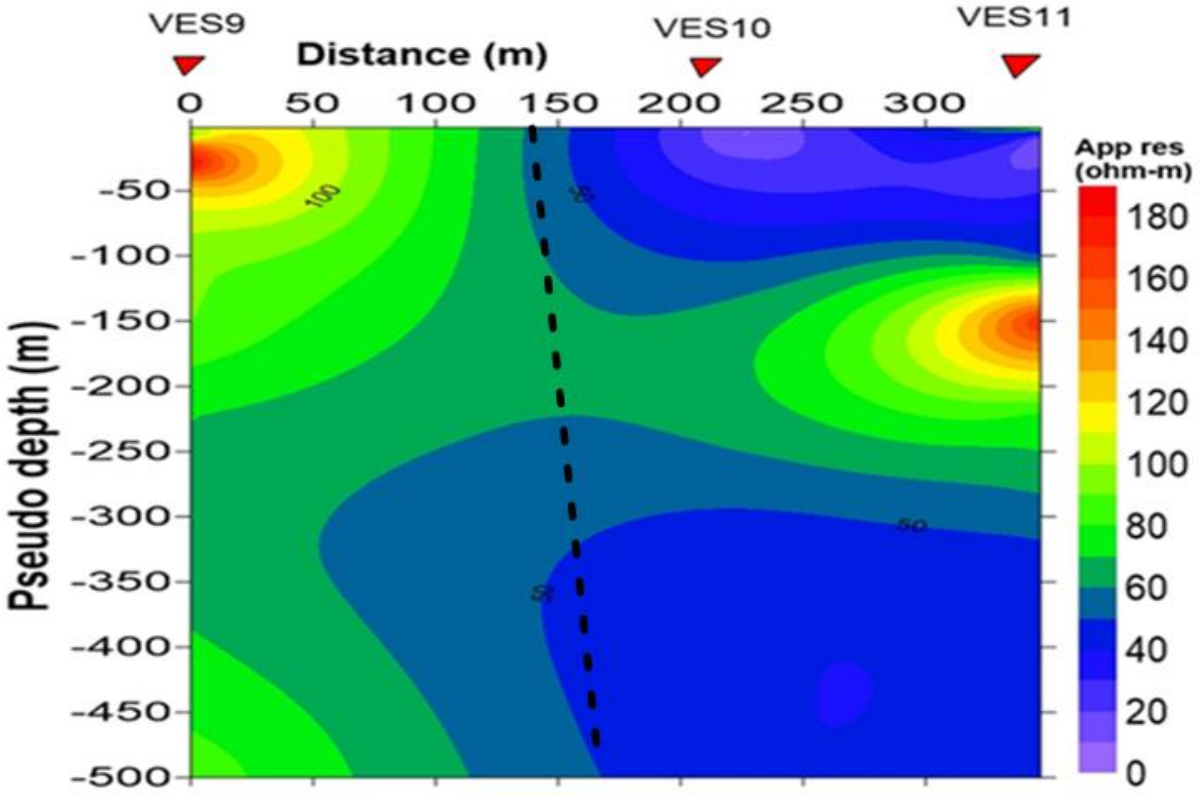

Figure 5. 10 Apparent resistivity pseudodepth section for Line-5.

5.3.10. Geoelectric Section of Line-5.

From the interpreted layer parameters of VES-9, VES-10 and VES-11 the resistivity sounding data are interpreted into layer parameters to construct the geoelectric section along Line-5 and the result is given in Figure 5.11. Four to five distinct geoelectric layers represent the subsurface, beneath the projected line. The resistivity of the upper most layer ranges between 7 to 77 Ω-m and have thickness 3 to 17m. It possibly represents the top dry and moist soil. Underlying the top layer, beneath VES-9 the subsurface is characterized by high resistivity ranging 222 Ω-m and has average thickness of 20m, which represents scoracous basalt with sand (correlate with the lithologic log of BH-1, which is called Misrak Anlemo). The third and fourth the geoelectric horizon having large lateral variation in resistivity with respect to the layer beneathbetween VES-10 and VES-11. In the other hand, the geoelectric layer between VES-10 and VES-11 is characterized by relatively low resistivity values. In Figure 5.11 inferred geological structures is shown by broken line. This broken line may reflects as geological fractured structures (normal fault) that exist between VES- 9 and VES-

10 up to a depth of 25-128m, which could bepossibly a good groundwater potential barrier.The last portion of the section mapped the low to moderate resistivity with the response of highly weathered/ fractured pumice/ volcanic ash beneath on VES-9, VES-10 and VES-11.

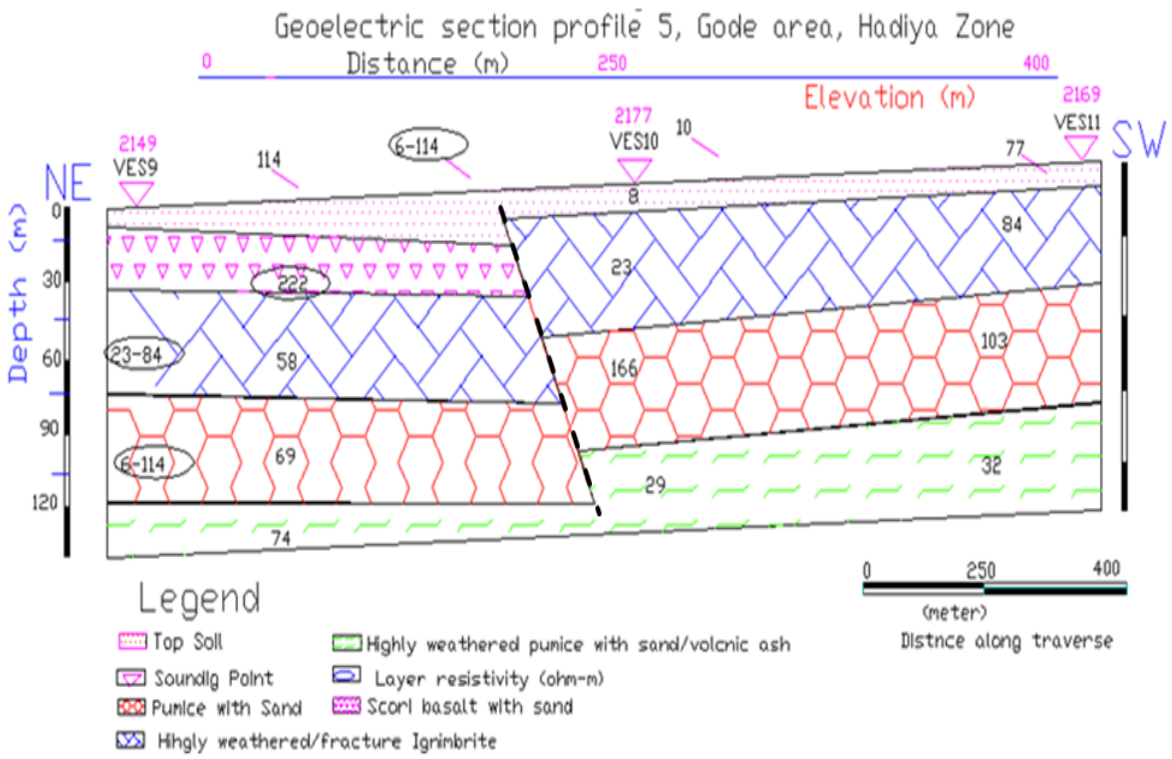

Figure 5. 11 Geoelectric section for survey Line-5.

5.3.11. Pseudodepth Section for Line-6.

The pseudo depth section constructed from apparent resistivity data of VES- 3, -7 and -12 that lie on survey line-6 is given in Figure 5.12. The projection line runs in NW-SE direction. According to this figure, there is a distinct lateral variation in resistivity with prominent low resistivity in the top and bottom zones mapped around VES-3 and VES-12.

The high resistivity zone is found in the region beneath VES-7 and some extend to VES-3. The vast region under the section shows extensive coverage of the moderate resistivity zone. The region beneath VES-3 and VES-12 the ground section is represented relatively conductive horizon, this low resistivity region are investigative for ground water potential.

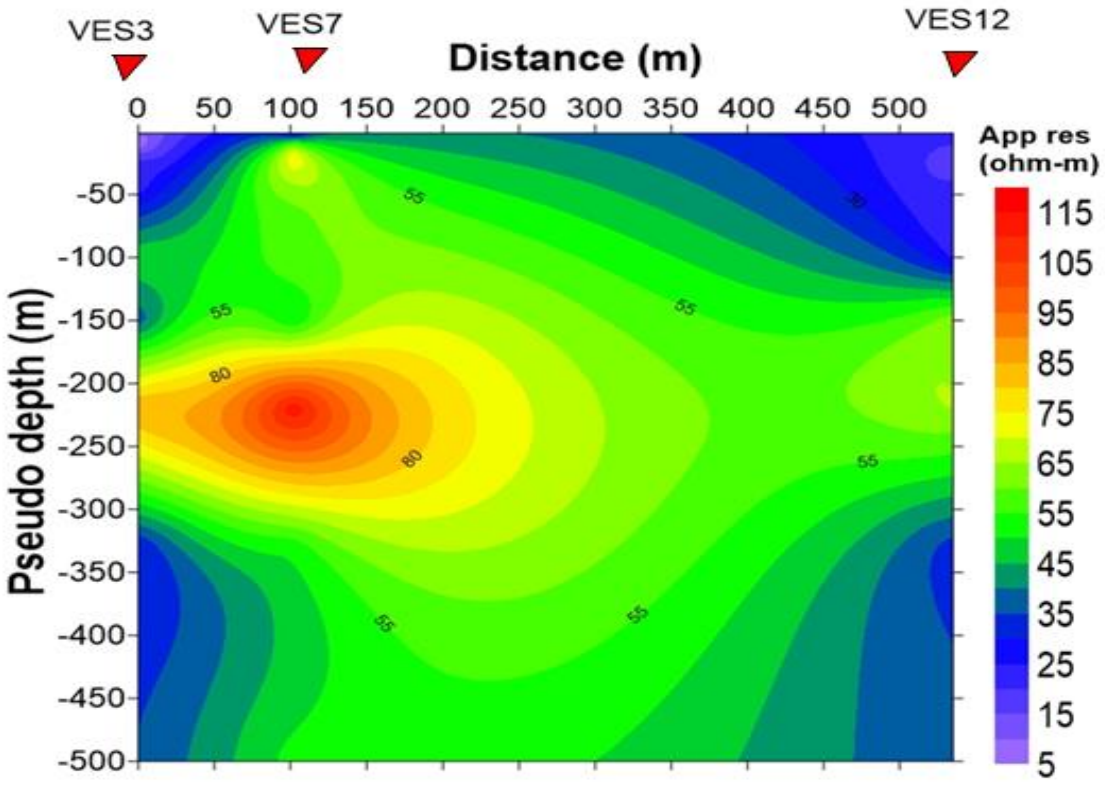

Figure 5. 12 Apparent resistivity pseudodepth section for Lline-6.

5.3.12. Geoelectric Section for Line-6.

The resulting geoelectric section constructed from the interpreted layer parameters of VES-3, VES-7 and VES-12 lying on this profile line six is given in Figure 5.13. From the geoelectric section, the sub surface consists of three geoelectric horizons. The topmost layer is a thin layer; its thickness varies from 2m at VES- 3 to 5m at VES- 12. Here the variation in resistivity values of first layer could result from the variation in moisture (water) content contained in the top soil of the wet muddy ground. Beneath the top layer, the second geoelctric of horizon coverers low to high resistivity value with resistivity ranges between (41 to 81 Ω-m). This layer attributes to geologically interpreted as weathered/ fractured ignimbrite underneath the section of all parts of VES- 3, VES- 7 and VES- 12.

The low resistivity (31-54 Ω-m) response of the third layer could be attributed to weathered pumice with sand/silt. The last portion of the section shows the low resistivity with the response of highly weathered/ fractured pumice beneath on the three VESs.

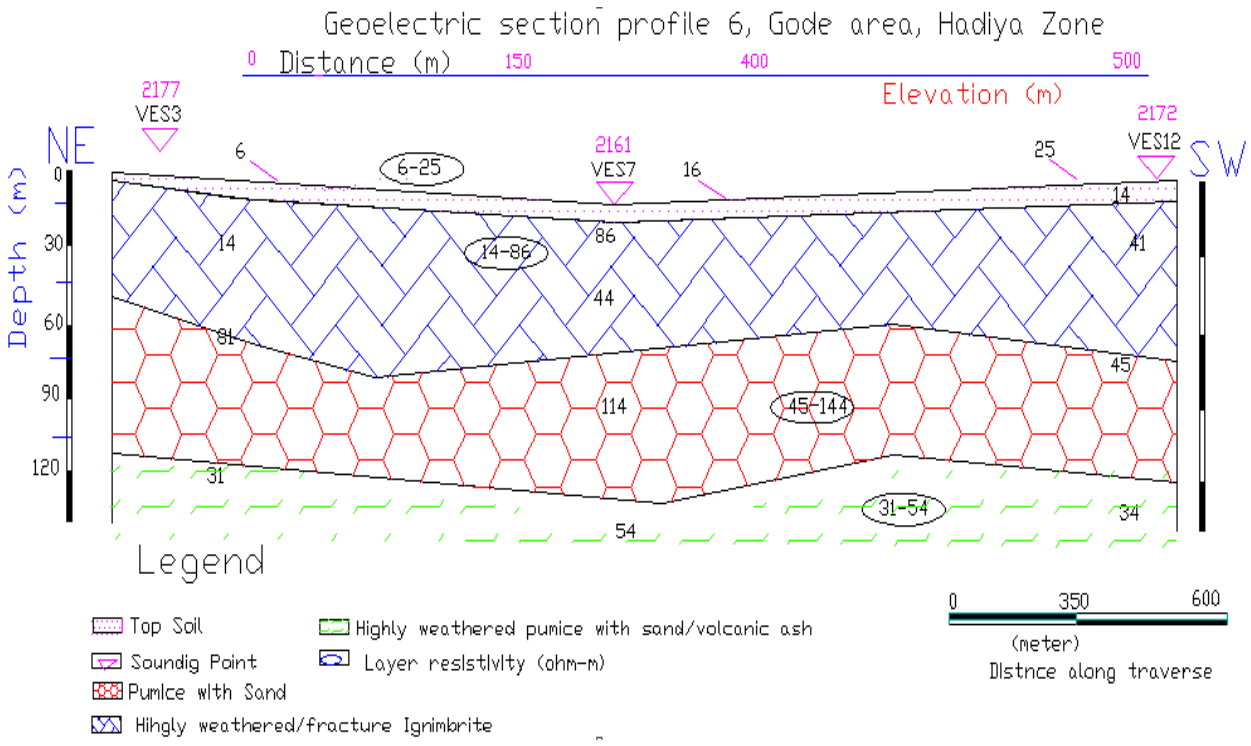

Figure 5. 13 Geoelectric section for survey Line-6.

5.4. Sliced-Staked Map for Different AB/2

The sliced-stacked map plot gives a visualization of the general picture of the subsurface electrical parameters and their variation both in the vertical and lateral directions. For this particular survey, the sounding points are seen to be well distributed over the area so that, it is possible to get a good representation of the ground overall.

The sliced stacked map shown in Figure 5.14 is constructed for AB/2=1.5, 20, 45, 220, 330, and 500m. The selection of such partition depends on the variability in subsurface resistivity distribution in order to show the horizontal variations of the resistivity at different pseudodepth sections. In particular, this representation shows the relative variation of the apparent resistivity value of the whole area both vertically and laterally at different depths of current electrode spacing. It is found that the resistivity value varies from 5-320 Ω-m.

According to the Figure 5.14 the most interesting feature of this slice-stacked plot is the low resistivity zone (<100Ω-m) that occupies the northwestern side of the survey and extends to the central portion of the area for all AB/2 values are the area worth considering. On the other hand, the relatively high resistivity zone (>100Ω-m) appears around the southwest

corner and the low resistivity zone dominates in all half current electrode spacing (AB/2) except at AB/2 =220m and AB/2 = 330m. The somewhat high resistivity region is masked by the low resistivity region by a narrow zone of intermediate resistivity values. Such narrow features are thought to designate geological structures, fault zones or contacts. Figure 5.14, in general shows clearly the areas where potential productive boreholes could be proposed as either or both the northwestern end (unconfined aquifer) or on the southeastern part (possibly confined aquifer) of the area.

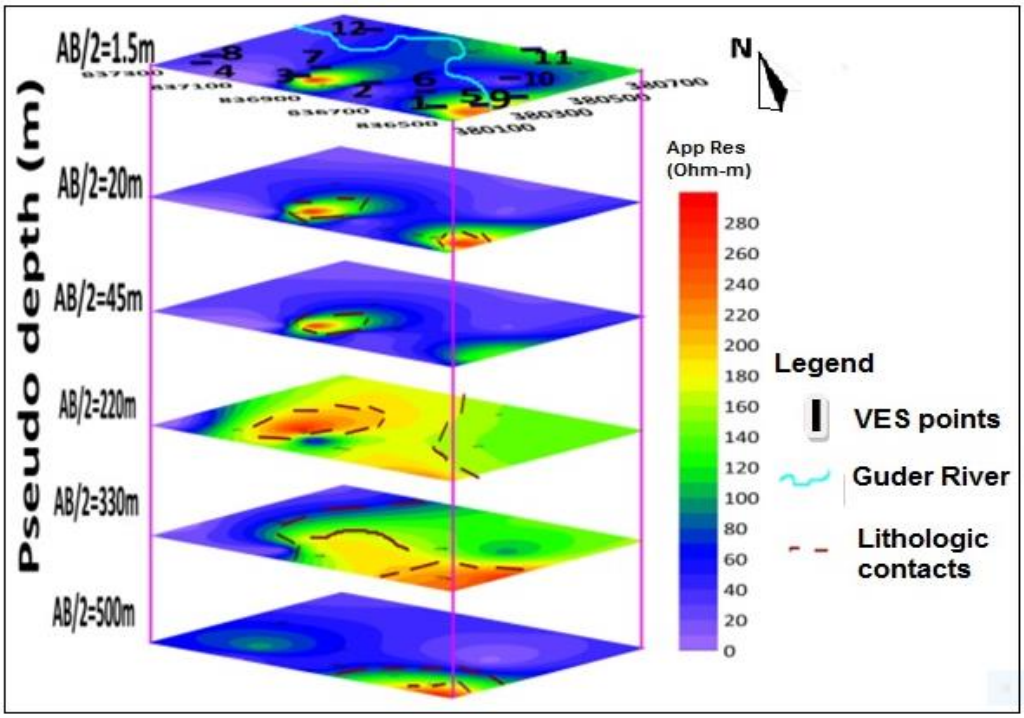

Figure 5. 14 Sliced-stacked map for different AB/2.

5.4. Characterization of Aquifer System

5.4.1. Isoresistivity layer map

The iso-resistivity plot for the current survey is as given in Figure 5.15, it is seen from the plot that the northeast and southeastern portion of layer shows a low resistivity region that could be interpreted as a potential groundwater zones due to the increased thickness of the aquifer specially in the region of VES-10 and VES-11. On the other hand, a relatively high resistivity zone appears around the southwest corner and around the central region. (see Figure 5.15).

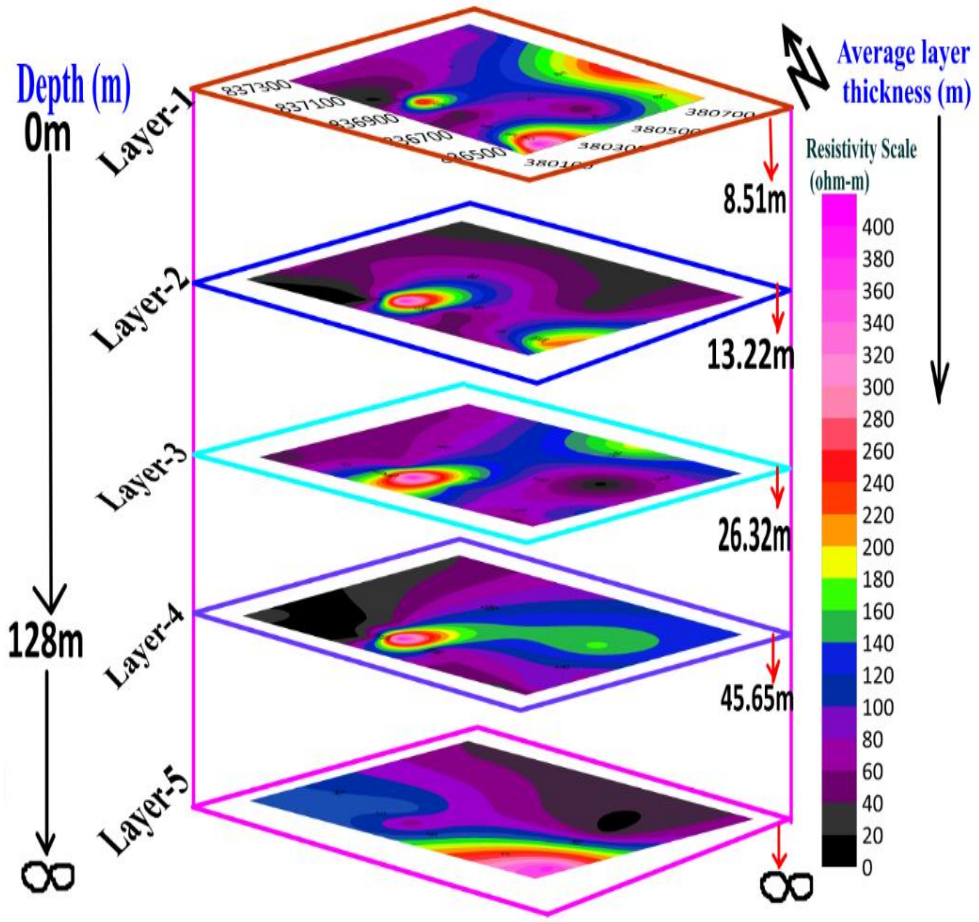

Figure 5. 15 Iso-resistivity map of the subsurface layers over the survey area.

5.4.2. Electrical anisotropy (λ) and Fracture porosity (φf)

A geo-electric layer is described by two basic parameters: resistivity (ρ_i) and thickness (h_i), where the subscript 'i' indicates the position of the layer in the section. Other geoelectric parameters like average transverse resistivity (ρ_t), average longitudinal resistivity (ρ_l) and coefficient of anisotropy (λ) can be derived from its resistivity and thickness (Henriet, 1976).

Now consider a prism shown in figure 5.16 that consists of 'i' parallel, homogeneous and isotropic layers of resistivities ρ_1, ρ_2, ρ_3, …,ρ_{n-1}, ρi, and thicknesses h_1, h_2, h_3, …, h_i respectively, For $i = 1, 2, ..., n$ layer, these parameters are described as given in Equations (5.1-5.5).

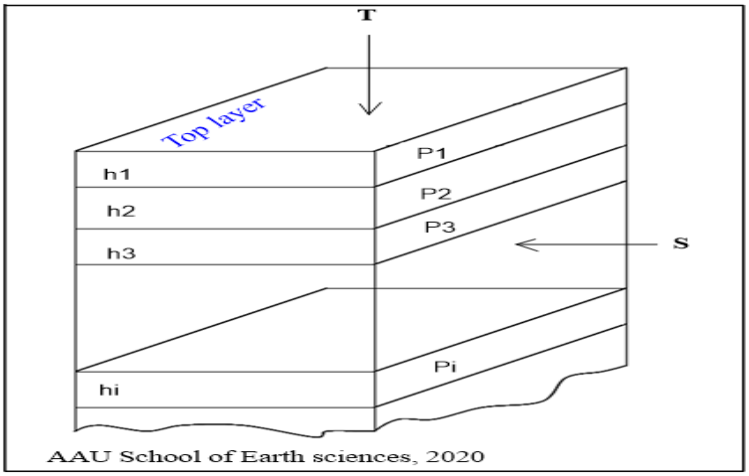

Figure 5. 16 A prism of unit cross section with resistivity 'ρ' and thickness 'h'

According to (Henriet, 1976) the coefficient of anisotropy can be derived as

Total longitudinal conductance (S) is defined as

$$S = \sum_{i=1}^{n} \frac{h_i}{p_i} \tag{5.1}$$

Similarly, the total transverse unit resistance (T) is also defined as,

$$T = \sum_{n=1}^{n} h_i p_i \tag{5.2}$$

$$p_l = \frac{H}{S} \tag{5.3}$$

$$p_l = \frac{T}{H} \tag{5.4}$$

The coefficient of anisotropy (λ) is given by,

$$\lambda = \sqrt{\frac{p_t}{p_l}} \tag{5.5}$$

Fracture porosities associated with tectonic fracturing of rocks were estimated using the expression derived by (Lane et al., 1995; Kumar et al., 2014).

$$\varphi_f = \frac{3.41\times10^{4}(N-1)(N^2-1)}{N^2C(\rho_{max}-\rho_{min})} \tag{5.4}$$

Where, φf is the fracture porosity; N is the vertical anisotropy related to the coefficient of anisotropy (λ). For Schlumberger 1-D data the vertical anisotropy is equal to the coefficient of anisotropy (λ) since, both λ and N are equal. The P_{max} is the maximum apparent resistivity (Ω-m); ρ_{min} is the minimum apparent resistivity (Ω-m) and C is the specific conductance of groundwater in mS/cm. The specific conductance of groundwater from boreholes and dug wells in this study area were averaged to 300 mS/cm.

A) Electrical anisotropy (λ)

As can be seen from Figure 5.17 an area with λ < 1.2 and up to 2 is considered to be a potential zone for groundwater including the northeast part of the map between VES-2, VES-3 and VES-4 the southwest region between VES-10 and VES-11. The dried BH-1, (Misrak Anlemo) found between VES-5 and VES-9, which attribute to a low water table fluctuation see (Figure 5.17). Thus, be adverse that the areas having minimum water table fluctuation is related with low λ values and higher water table fluctuation regions are associated with high λ values (Shailaja1, G. 2016).

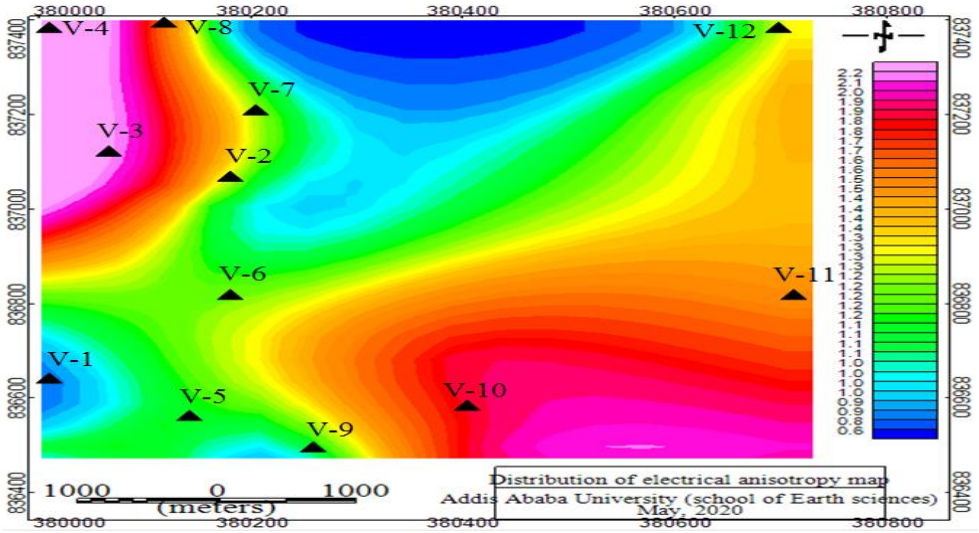

Figure 5.17: Distribution of electrical anisotropy for the surveyed area.

B) Fracture porosity (φf)

As mentioned earlier in the geoelctric section shown Figure (5.9 and 5.11) very famous joints and fractures revealed in the survey area enhances secondary porosity. The estimated fracture porosity (φf) reveals that porosity values are low on the middle portion of the study area.on the other hand a very low fractured area mapped at north side and to some extent in the southeastern (VES 1, 5, 6 and 9) part of the study area the study area (Figure 5.18). A maximum porosity value of (18.7% -71%) was observed in the southwestern and eastern part of the study (VES-2, 3, 10, and 11) infer to the presence of a maximum groundwater potential aquifer specifically, between VES-10 and VES-11. To assure this system, the previous drilled borehole-2, (Tachegnaw Gode), which is found near to VES-3 really it, has a good groundwater potential aquifer and applicable to the society.

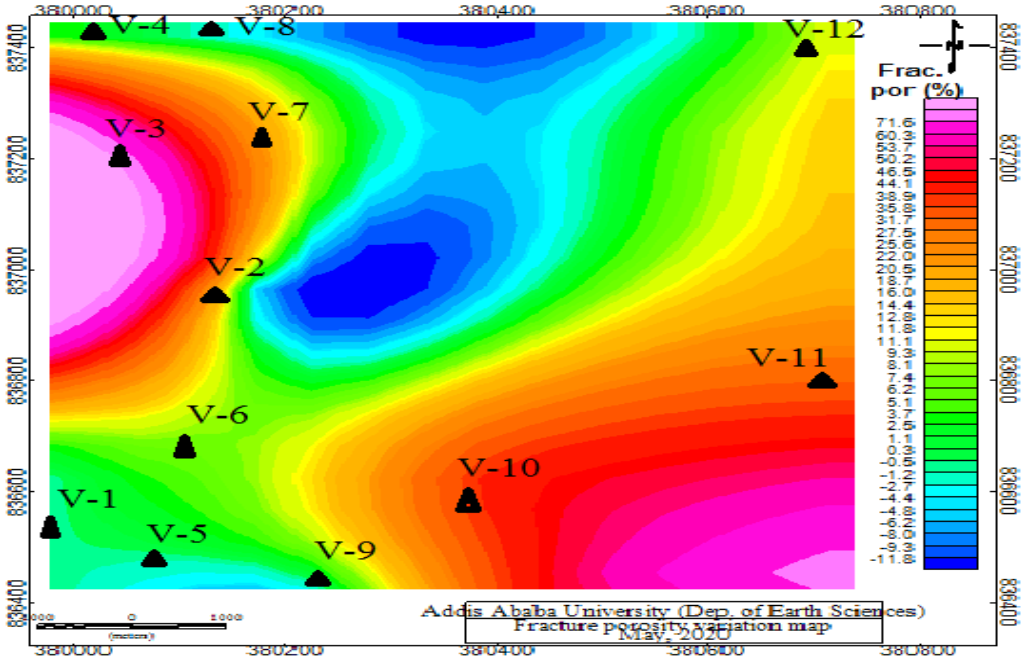

Figure 5. 17 Fracture porosity variation map for the surveyed area.

5.5. Magnetic data results and interpretation

The basis of magnetic survey in this study is to identify and describe the subsurface structures contribute to groundwater flow that is associated with anomalous regions in the survey area along Guder River. The new version, Oasis Montaj (Geosoft v 6.4.2) were used for interpret the magnetic data. In the following sections, briefly present and discuss them separately.

5.5.1. Total magnetic field intensity map

The total magnetic field intensity map (Figure 5.19) of the study area is compiled by plotting all the magnetic data that are corrected for diurnal variation at their respective locations. Figure 5.19, the northeastern and southwestern part of the surveyed area, shows very low magnetic anomaly relative to the other region part of the study. The region where the subsurface rock units are highly affected by the presence of thick soil cover and/or the presence of weak zones filled with weathered material. While a large portion of the survey area in the northeast direction is characterized by low to intermediate magnetic anomaly response and is due to slightly and moderately weathered/ fractured rock units.

The central portion the map show the high values of magnetic anomalies depicts regions of very high magnetic anomaly response resulting from the presence of highly magnetized bodies that beneath the surface. This could be fresh ignimbrites/ scoraceous basalt found at a relatively shallower depth, which is towards to the northeast part of Guder River. The black dots are indicates the magnetic data distribution of the survey area, while The base-station location represented by (black-triangular shape) shown in the map (Figure 5.19) was chosen to be free of geomagnetic noise, away from steel objects, vehicles and electrical power lines, which could interfere with recording of the diurnal variations.

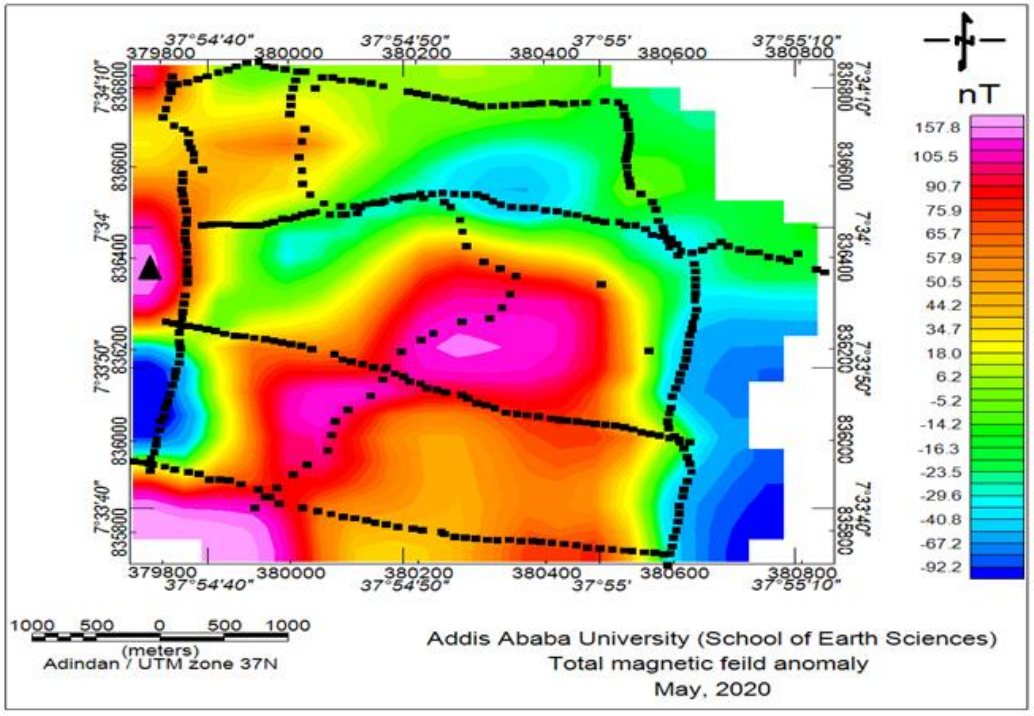

Figure 5. 18 Total magnetic field anomaly map of the study area.

5.5.2. Regional–Residual magnetic anomaly separation and data enhancement

Separation of regional and residual anomaly components is important to see the effects of deep seated and shallow depth sources contributing to the anomaly as briefly shown in (Figure 5.20 and 5.21).

I) Regional magnetic field anomaly map

The regional magnetic anomaly map of the study area was generated by applying a low pass filtering technique using the Oasis Geosoft Montaj Software (v 6.4.2). The high magnetic

anomaly zones observed over the study area is the response of deep seated high susceptibility volcanic rocks.

In particular, the magnetic anomaly is very high over the central and northeastern part of the map, and an intermediate magnetic anomaly observed in the north and extends to the southeast part of the area. Whereas, very low magnetic susceptibility observed in the eastern end part of the map see (Figure 5.19).

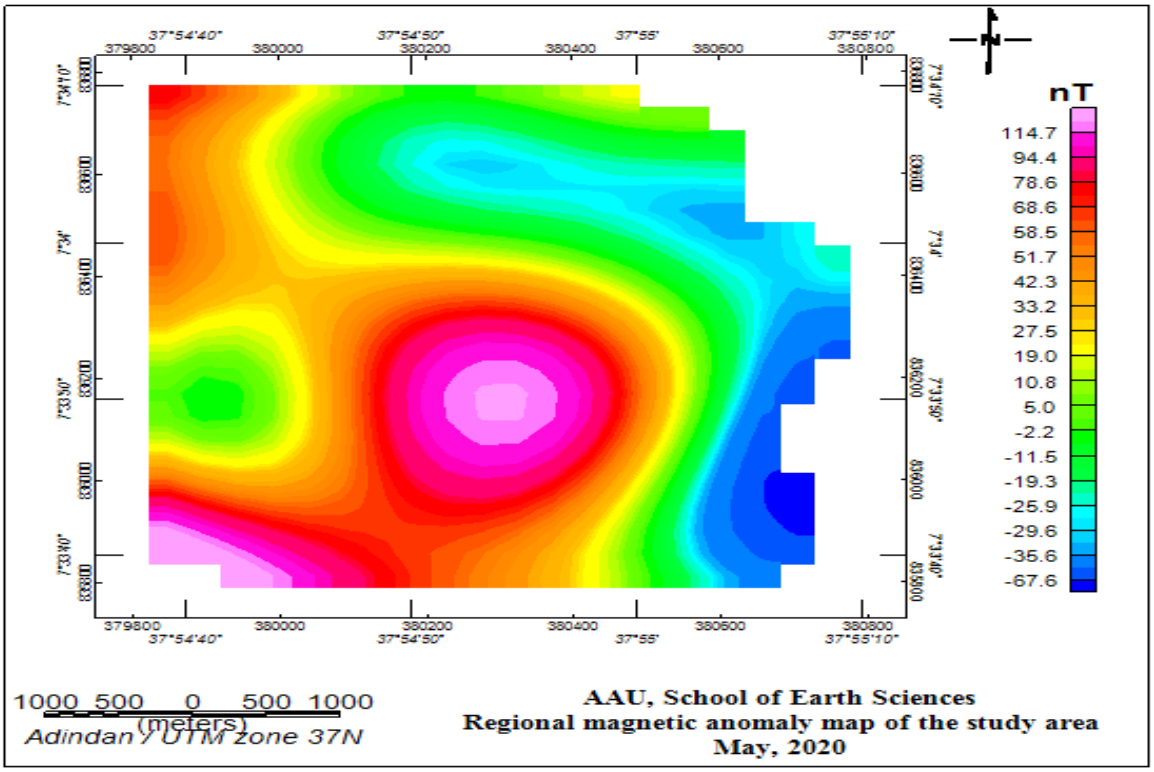

Figure 5. 19 Regional magnetic anomaly map of the study area.

II) Residual magnetic field anomaly map

A high-pass filter is used to obtain the residual anomaly. The prominent geological features observed in the residual magnetic anomaly map are generally preserved in the total and regional magnetic anomaly maps (Figs.5.19 and 5.20). The high magnetic susceptibility sediments derived from the neighboring volcanic rocks. Field observations indicate that the observed residual magnetic anomalies are also governed by the distribution of geologic materials and structural features. Areas covered by scoracous basalt and/or massive ignimbrites are associated with positive magnetic anomalies.

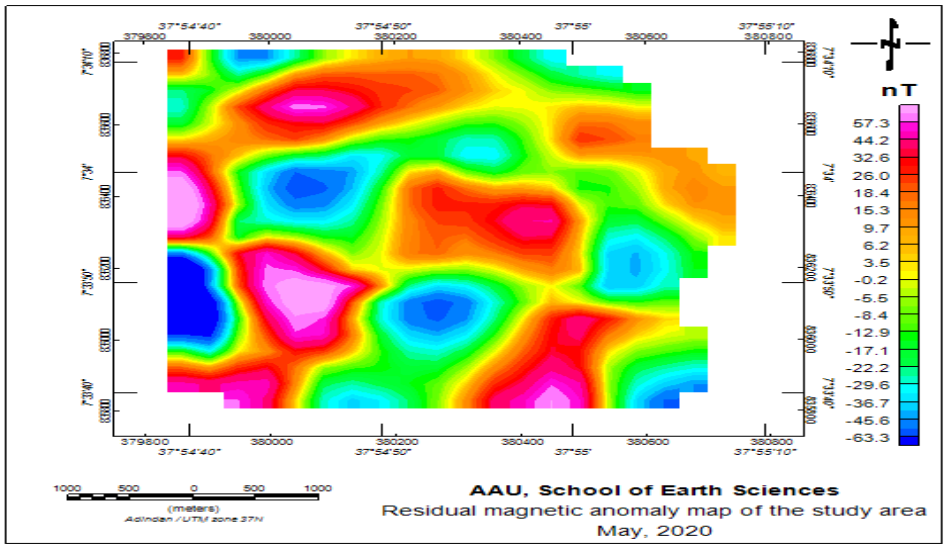

Figure 5. 20 Residual magnetic anomaly map of the study area.

The plot (Figure 5.21) illustrates the typical reduction in energy with increase wavelength, which shows the deep source of (regional anomaly) mean average depth at about 5km and the shallow source of (residual anomaly) mean average depth detect up to 500m of the study area.

III) Reduce to magnetic pole map

The obtained RTP anomalies (Figure 5.21) were shifted south and northwards, with the same general trend to residual anomaly map, but with clear shapes and well-separation from their background. Their overall amplitudes were obviously increased.

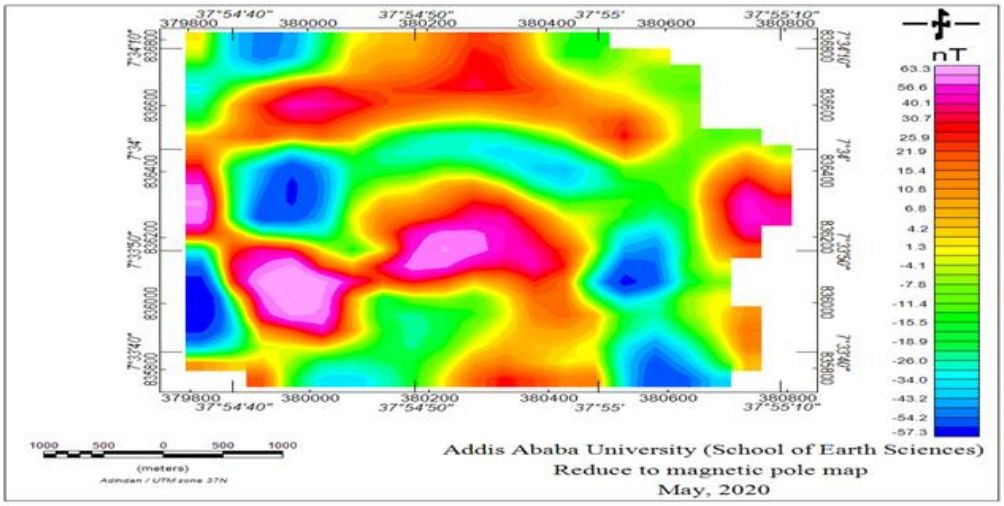

Figure 5. 21 RTP magnetic anomaly map of the study area.

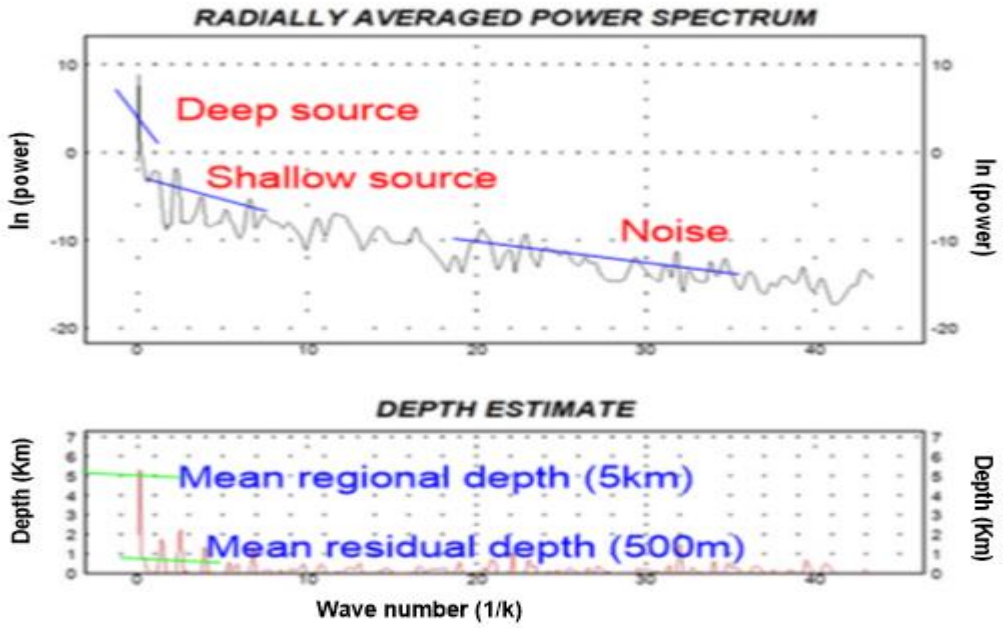

Figure 5. 22 Power spectra of the corresponding averaged depths to the regional and residual magnetic anomaly source of the study area

5.6. Data enhancement

Data enhancement techniques of potential field data (mostly, residual magnetic anomaly field data) are a significant method that are employed for highlighting the contrast of magnetic anomalies generated by deep-seated and shallow origin anomalous geologic bodies. The common used data enhancement techniques including the analytical signal method, Euler depth method and tilt derivative method are employed here. As a result, the analytical signal magnetic map (Figure. 5.23), the tilt derivative magnetic map (Figure. 5.24) and the Euler depth magnetic map (Figure. 5.25) are produced from values of the residual magnetic anomaly map (Figure. 5.19) compiled for this study.

5.2.6 Magnetic analytical signal map

The analytical signal map shown in (Figure 5.23) was developed from the magnetic anomaly map over the causative bodies. The analytical signal has a form that depends on the locations of the bodies but not their directions of magnetization, and is always positive. The map reveals magnetic anomalies that result from vertical and horizontal variations/ contacts of geologic structures. The large area cover analytic signal gradients as compared with the

surrounding sediments and low magnetic susceptibility rock units like tuff and other pyroclastic volcanic rocks. Ones notice that as can be observed from the map, the maximum values of the analytic signal map are generally coincident with the magnetic anomaly peaks observed in the residual magnetic anomaly overall in the northeast and southwest part of the study area. In fact, there are also some contacts of lithologic unit shown in figure (5.23), the yellow solid dashed lines represent the possible structure of contact zone, while the smooth white line shows the possible lithological weak zones/ fractures. Therefore, the geologic contacts are possibly attributed to the variation in the magnetic susceptibilities of the different geologic units (intrusive bodies, country rock, and structural contacts).

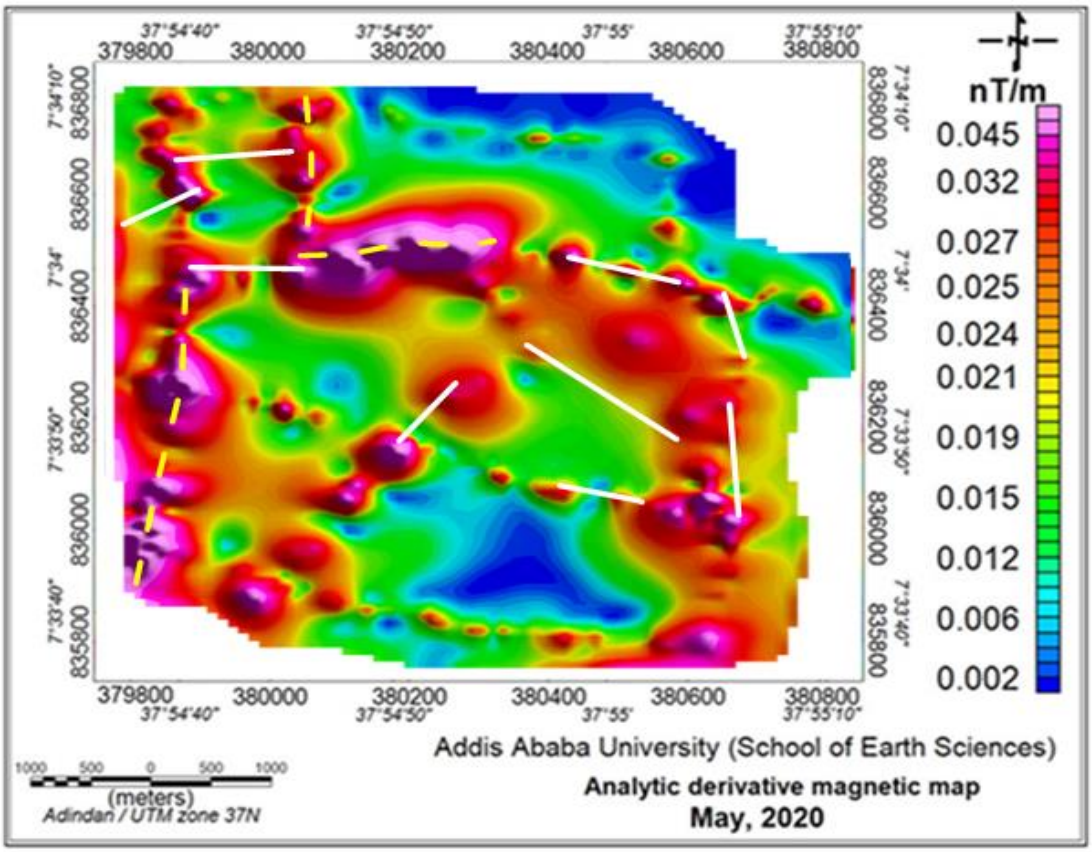

Figure 5. 23 Analytic signal magnetic map of the study area.

5.2.5. Tilt derivative magnetic map

From the analytical signal map again it is also possible to create the tilt derivative map as shown in the Figure 5.23. The tilt angle has the attractive property of being positive over sources, cross through zero at or near the edge of a vertical side source and is negative

outside the source region (Miller and Singh, 1994). Accordingly, the study area is characterized by numerous structures/contacts oriented in the NE-SW and NW-SE directions. Overall,as shown in the Figure (5.24)the black solid dashed lines represent the possible structure of contact zone and the smooth white line shows the possible lithological weak zones/ fractures whereas, the red solid line indicates out of the source of magnetic field in the study area.

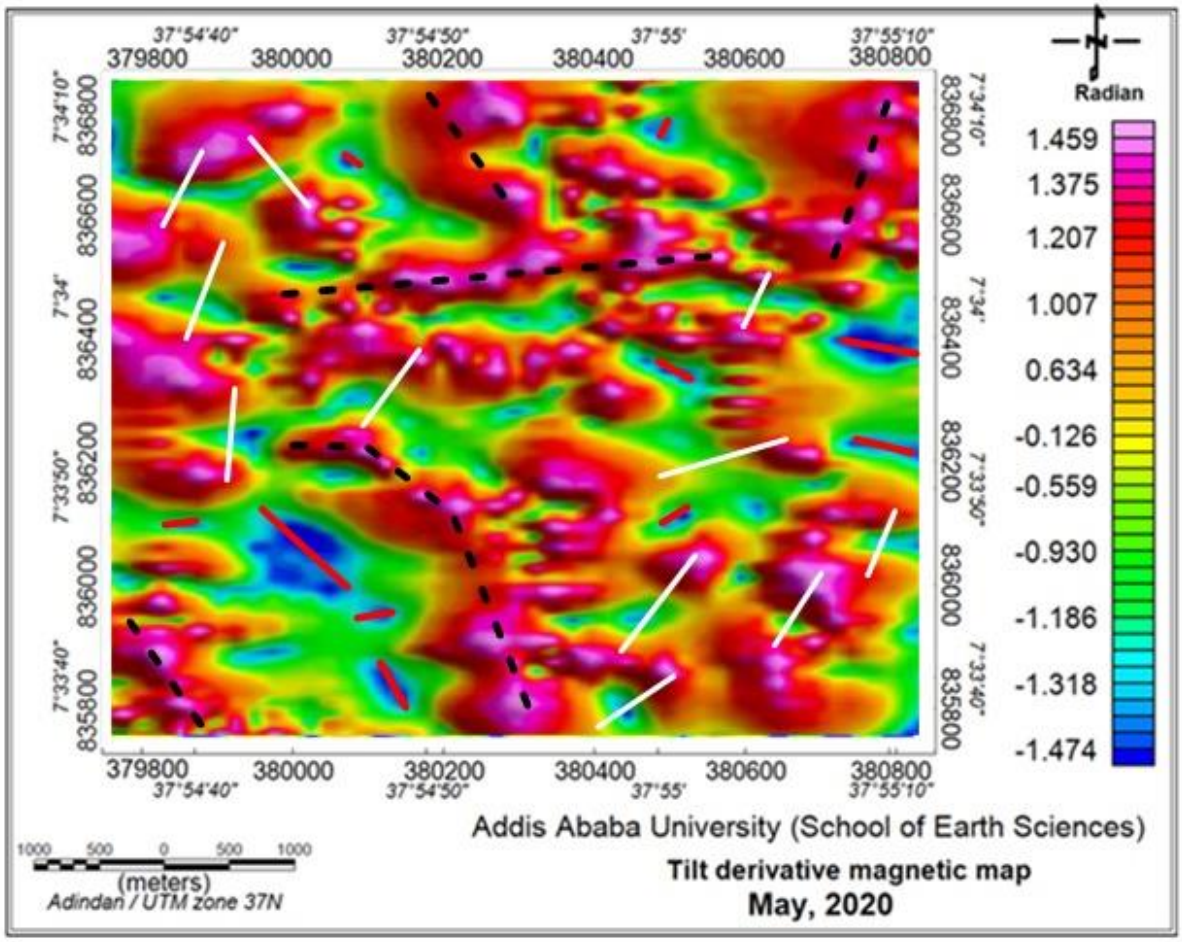

Figure 5. 24 Tilt derivative of magnetic map of the study area.

5.2.6. Euler deconvolution magnetic map

Euler deconvolution technique is applied to the total magnetic anomaly in order to estimate the depth and location of the magnetic source. In standard Euler deconvolution process, each model contains solutions of a particular structural type defined by a structural index. From the principle of Euler deconvolution, the structural index values 1, 2, 3 represent geological features of contact, vertical pipe/horizontal cylinder and sphere respectively. Figure 5.24 Euler deconvolution magnetic map for SI = 1 of the study area.

The map reveals magnetic sources of different depths marked by different colored symbols plotted on the map. These include a yellow, radish and pink color circle indicating magnetic sources with depth less than 150m. The red circle indicates magnetic sources that range from 150 to 250m depth. The green circle represents sources that range from 250 to 350m depth. The blue circle represents sources that range from 350 to 450m depth. The light green circle represents sources that are greater than 450m. This representation has been interpreted as being due to existence of structures (weak zones) that contain highly magnetized bodies shown in the map of the given (Figure 5.24) in the southeast flank of the current study area. As result, it is recommendable that relatively southwest flank is high bearing capacity than northeast side of the area for groundwater point of view.

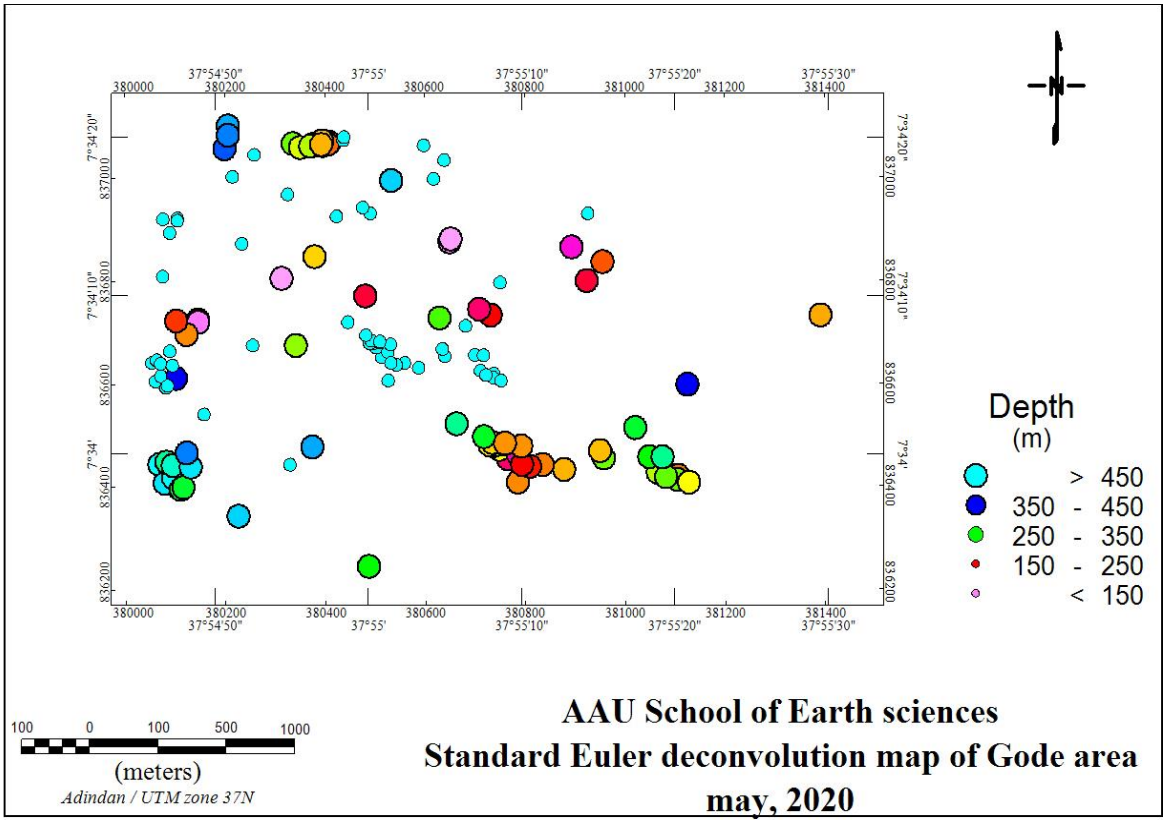

Figure 5. 25 Euler deconvolution magnetic map for SI =1 of the study area.

5.4.2. 2D Magnetic model along Line-6.

The 2D magnetic model is constructed using the GM-SYS modeling software and it is a very essential to estimate the physical properties of the subsurface geological units. Any difference between the model response and the observed magnetic field are reduced by refinement the model structure.

It should be noted that magnetic model is non-unique, many Earth materials can produce the same magnetic response and several lithologies may be interpreted from a given model block's magnetic susceptibility. The magnetic 2D model is developed from magnetic anomaly of profile one with interpreted VES curve parameters of the geoelectric section of VES-7, VES-6, VES-5 and VES-2. As shown in Figure 5.26 the model reflects that existence of weak zone (fracture/ fault) below depth of 25m that extend to 230m depth. Lithologic unit that are described in the model includes: top soil, ignimbrite, pumice, volcanic ash and underlying scoracous basalt.

Geoelectric section along this profile as shown in Figure 5.9 reflects the same lithologic units and geological structures except slight variation in thickness. Based on the geoelectric section and lithologic log of the borehole ignimbrite, pumice and basalt are varying in their degree of weathering and fracture. Groundwater system of the area is controlled by highly weathered and fractured horizons and geological structures.

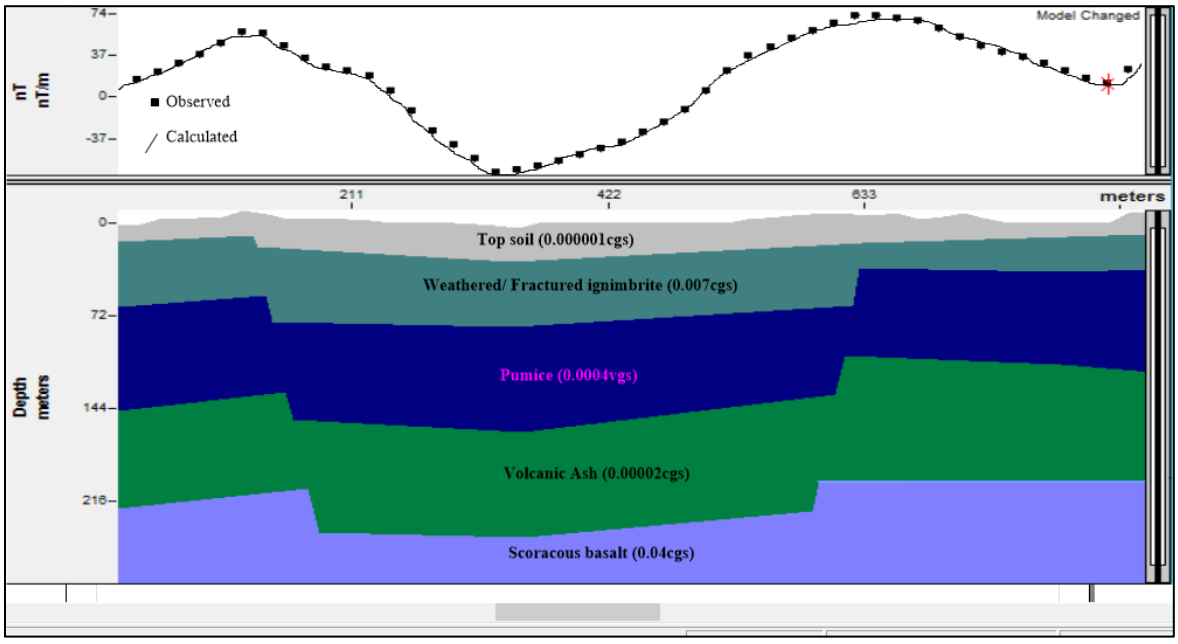

Figure 5. 26 2D modeling of magnetic data along Line-6.

CHAPTER SIX

CONCLUSIONS AND RECOMMENDATIONS

6.1. Conclusions

Based on the investigations made in this study the following conclusions and recommendations are forwarded.

Vertical electrical sounding (VES) and magnetic survey data collected over a number of selected profiles and at random points (for the magnetic) have been used to investigate ground water potential along the Guder River in Gode area, just north of Hosanna town. A total of 12 VES points along six traverses with maximum half-current electrode spacing (AB/2) of 500m have been conducted. Magnetic data of about 405 reading points are also collected in systematic manner along seven profiles that run over the six resistivity (VES) traverses and additionally over random points designed to cover the area of study as much as possible. The magnetic data were collected at 10 m station spacing for those conducted on the VES survey lines and about 20 m for the random points. The electrical data have been presented in the form of apparent resistivity pseudo depth and geoelectric sections as well as data enhancement schemes like anisotropy and fracture porosity. On the other hand, the magnetic data have been corrected and presented in the form of total field magnetic anomaly maps, regional and residual plots, analytic signal map, tilt derivative and Euler deconvolution techniques. Based on the results of the geophysical surveys presented thus, their respective interpretations and available information from additional sources like borehole litholgic logs, the following conclusions are drawn.

The apparent resistivity pseudo-depth section, sliced-stacked map and the geoelectric sections show presence of low resistivity horizons at different depth with their physical suitability to act as aquifer beds. The aquifer thickness in the area is obtained to 45m to 92m. The study result revealed that highly weathered and fractured ignimbrite/ pumice with sandy soil is the main water bearing horizon which has good groundwater potential specially, between VES-10 and VES-11. Sliced-stacked section constructed from VES data showed the presence of highly conductive horizons (saturated zone), specifically in eastern direction of the study area.

As shown in the geoelectric sections and 2D magnetic profile plots, the area is transected by several subsurface geological structures (discontinuities), especially in the northeast and southwest part of the area that are important for groundwater flow and occurrence. 2D magnetic model reflects existence of normal fault below depth of 25m that extend to 230m along the survey lines VES-5, VES-6, VES-2 and VES-7. Comparison of the geophysical results with borehole lithologic data shows that results of geophysical interpretations are well correlated with the borehole lithologic log. Geological translation of the VES survey in the geoelectric section (Figure 5.9) is attributed to the same subsurface stratigraphy within in the 2D magnetic modelling (Figure 5.26). Integrated geophysical method has facilitated the data interpretation and greatly reduced the ambiguity in each method.

6.2. Recommendations

Based on the limitation and results obtained from this study, the following points are recommended.

- The data analysis four well sites are highly recommended for drillingin the neighborhood of three VES points, VES- 2, VES- 3, VES-10 and VES-11 this is the response of fractured layer beneath in the subsurface of the study area.
- The study area is highly controlled by geological structures or weak zones to govern the movement and flow of groundwater, so that care must be taken in the drilling stage.
- For fast, cost effective and accurate result in hydrogeological investigations integrated remote sensing and GIS approach is highly recommended.
- It is highly recommended that to study detailed time domain electromagnetic survey and geochemistry for the investigation of additional drilling point and the quality of the groundwater in the area.
- It is recommended that to study detailed structural geological investigations for mapping the orientation of faults, fractures and weak zones as well as their natures like dip, strike and their extension.
- Further regional hydrological and hydro-geological investigations are recommended to understand the basin, amount of precipitation and evaporation, which are used to estimate the percolation of surface water to the groundwater.

REFERENCES

Araffa, S., Adel, M. and Fernando, S. (2017). 3-D VES inversion and shallow seismic refraction techniques for delineating groundwater and subsurface structures at the Northwestern part of the Gulf of Suez, Egypt. *Egypt J Pet.*,**26**(2):457–475.

Bakheit, A.A., Sansy, M.A., Riad, S., Omran, A.A., Ibrahim, H.A., 1993. Application of the resistivity method to study ground water potentialities on a part of the entrance of Wadi El-Assiuti, Eastern Desert, Egypt. *Qatar. Univ., Sci. J.***13** (2), 341–347.

Bernard, J., Vachette, C. and Valla, P. (2003). Deep groundwater survey with audio magnetottelluric soundings: Annual Meeting Abstracts, Society of Exploration *Geophysics*, **52**: 31-85.

Bitsiet Dereje and Dessie Nedaw (2018). Groundwater recharge estimation using wet pass modeling in upper Bilate catchment, Southern Ethiopia, *Momona Ethiopian Journal of Science*, Mekelle University, **11**(1): 37-51.

Brewster, M.L., Annan, A.P., Greenhouse, J.P., Kueper, B.H., Olhoeft, G.R., Redman, J.D. andSander, K.A. (1995). Observed migration of a controlled DNAPL release by geophysicalmethods. *Groundwater*,**33**:977-988.

Choudhury, K., Saha, D.K., and Chakraborty, P. (2001). Geophysical study for salaine water intrusion in a coastal alluvial terrain, *J. Apllied Geophy.*, **46**: 189-200.

Corti, G. (2009). Continental rift evolution: from rift initiation to incipient break-up in the Main Ethiopian Rift, East Africa. *Earth Sci. Rev*.**96**: 1-53.

Dobrin, M. B. (1976). Introduction to Geophysical Prospecting. Cambridge University Press. New York, McGraw-Hill. 630 pp.

Ebinger, C. (2005). Continental breakup: the East African perspective. *Astronomy and Geophysics*,**46 (2)**: 16–21.

EIGS, (1993). Hydrogeological map of Ethiopia. A report on Geology, geochemistry and gravity survey of Hosanna area. Unpublished report, Addis Ababa, Ethiopia.126 pp.

Elewa, H. H., (2008). Prediction of future drawdown of water levels of the Pleistocene aquifer system of Wadi El-Assiuti Area, Eastern Desert, Egypt, as a criterion for management and conservation. *Resources, Conserv. Recycl.*,**52**:1006–1014.

Everett, M.E. (2013). Near-surface applied geophysics, Cambridge University Press. McGraw-Hill, New York, USA, 837 pp.

Farrag, A.A., Riad, S. and Ahmed, M. H. (2002). Groundwater situation and evaluation in the Nile basin east of Assiut, Egypt. *J. Engin. Sci*., Assiut Univ **30** (2):517–542.

Farrag, A., Ebraheem, M., Sawires, A. and Ibrahim, N. (2019). Petrophysical and aquifer parameters estimation using geophysical well logging and hydrogeological data, Wadi Assiuoti, Eastern Desert, Egypt. *Journal of Africa Earth Sciences,***149**: 42-54.

Flathe, H. (1955). Possibilities and Limitations in Applying Geoelectrical Methods to Hydrogeological Problems in the Coastal Areas of North west Germany. *Geophysical Prospecting*, **3**:95-110.

Flathe, H. (1970). Interpretation of Geoelectircal Rsistivity Measuremnts for Solving Hydrogeological Problems. In Morely, E. W. (ed.), Mining and Groundwater Geophysics: Geological Survey of Canada, *Economic Geologica* Report, **2**: 580-597.

Gebremedhin Berhane., Samuel Kebede and Tesfamichael Gebreyohannes, (2015). An integrated approach for detection and delineation of leakage path from Micro-Dam reservoir northern Ethiopia, *Eng. Geol. of Belgium***2**:10-21.

Giday Woldegabriel, Aronson, J. and Walter, R.C. (1990). Geology, geochronology and rift basin development in the central sector of the Main Ethiopian Rift. *Geol. Soc. Amer. Bult.* **102:**439–458.

Haile Arefayne and Semir Abdi (2016). Groundwater Exploration for Water Well Site Locations Using Geophysical Survey Methods. Hydrol, **7**: 226. doi:10.4172/2157-7587.1000226.

Hassanein, H., El-Kaliouby, H., and Al-Garni, M.A. (2007). The use of DC-resistivity to outline the subsurface hydrogeological and structural setting beneath a proposed site for subsurface dam building, Makkah Al- Mukarramah, Saudi Arabia, Journal of King AbdulAzizUniveristy: *Earth Sciences*, **18**: 117-138.

Henriet, J.P. (1976). Direct application of Dar-Zarrouk parameters in ground water surveys, *Geophys. Prospect*, **24**:344–353.

IGRF (2010).IGRF model field 11th generation, online calculator. International Geomagnetic ReferenceFieldAvailability *http://www.ngdc.noaa.gov/IAGA/vmod/igrf.html.*

Imran, A., Sankar, K and Dar, A. (2010). Remote sensing technology and geographic information system modeling: an integrated approach towards the mapping of groundwater potential zones in Hardrock terrain, Mamundiyar basin. *Jour. of Hydrology*, **394**:285-295.

Ishola, K., Ogunsanya, S. Adiat, K. and Abdulrahman, A. (2013). Assessing groundwater potential zones in basement complex terrain using resistivity depth soundings: a case of challenge in Ibadan, southwestern. *Nigeria Journal of Science,***1**(1):11-32.

Israil, M., Mufid, A. and Singhal, C. (2006). Application of a resistivity survey and geographical information system analysis for hydrogeological zoning of a piedmont area, Himalayan foothill region, India. *Hydrogeology Journal*, **14**:753-759.

Jackson, P.N., Taylor, S.D. and Stanford, P.N. (1978). Resistivity, porosity and particle shape relationships for marine sands, *Geophysics*, **43**:1250-1268.

Kumar, D., Rai, S.N., Thiagarajan, S., and Ratnakumari, Y.(2014). Evaluation of heterogeneous aquifers in hardrocks from resistivity sounding data in parts of Kalmeshwar taluk of Nagpur district, India, *Current. Science,***107** (7) pp: 1137-1145.

Lane J, J.W., Haeni, F.P., and Watson, W.M., (1995). Use of a square array direct current resistivity method to detect fractures in crystalline bedrock in New Hampshire, *Ground Water resource,* **33** (3): 476–485.

Kaya, G.K. (2001). Investigation of groundwater contamination using electric and electromagnetic methods at open waste-disposal site, a case study from Isparta, Turkey, *Environ. Geol*., **40**:725-731

Kazmin, V., Seife Michael Berhe, Nicoletti, M. and Petrucciani, C. (1980). Evolution of the northern part of the Ethiopian Rift. Accad. Naz. Lincei, Rome, **47**: 275–291.

Kearey, P. Brooks. M. and Hill, I. (2002). An introduction to geophysical exploration, 3rd ed., Blackwell Science Ltd. 160 pp.

Kossinski, W.K. and Kelly, W.E. (1981). Geoelectric sounding for predicting aquifer properties, *J. South Afr. Groundwater,* **19**:163-171.

Lashkaripour, G.R.; Sadeghi, H. and Qushaeei, M. (2005). Vertical electrical soundings for groundwater assessment in southeastern Iran: *J. Applied Geophy*., **5**: 973-977.

Loke, M.H. (2001). Electrical Imaging Survey for Environmental and Engineering Studies: A practical guide to 2D and 3D surveys in Germany using near surface geophysics, *Journal of Applied Geophysics*,**84**:77–85.

Maillet, R. (1947). The fundamental equation of electrical prospecting, *Geophysics*, 12: 529–556.

Mazac, O.; Benes, L.; Landa, I. and Maskova, A. (1990). Determination of the extent of oil contamination in groundwater by geoelectrical methods in Ward. *Geotechnical and environmental geophysics, Society of Exploration Geophysicists,***2**: 107-112.

Milsom, J. (2003). Field Geophysics. John Wiley & Sons Ltd, London, England, 3rd edition. 249 pp.

Ministry of Water and Energy (MOWE) (2014). Water Source Assessment, Feasibility Study and Preliminary Design for 12 Rural Kebeles and 3 Rural Towns Water Supply in Hosanna and Lemo Woredas. V-I. Unpublished technical report. Addis Ababa, Ethiopia.

Niwas, S., and Celik, M. (2012). Equation estimation of porosity and hydraulic conductivity ofRuhrtal aquifer in Germany using near surface geophysics, *Journal of Applied Geophysics,***84**:77–85.

Reynolds, J.M. (1997). An Introduction to Applied and Environmental Geophysics. India *Journal of Indian Geophysics,* **20 (**5):453-461.

Seifu Kebede (2010). Groundwater in Ethiopia Springer Heidelberg New York Dordrecht London ISBN 978-3-642-30390-6.

Shaaban, F. (2002). Vertical electrical for groundwater investigation in northwestern Egypt: a case study in a coastal area, *J. African Earth Sci.*, **33**:673-686.

Slichter, L.B. (1929). Certain aspects of magnetic surveying. *American Institute of Mining and Metallurgical Engineers, Transactions*, **81**:238-260.

Sintayehu Legesse (2009). Integrated hydrogeological investigation of upper Bilate River catchment: Unpublished M.Sc. thesis, Addis Ababa University, Ethiopia. 95 pp.

Srinivasa R, Y., Reddy, T. and Nayudu, P. T. (2000). Ground water targeting in a hard rock terrain using fracture pattern modelling, Niva River basin, Andhra Pradesh, India, *Hydrogeology Jour.*, **8**:494-502.

Sultan, A. (2016). Delineation of groundwater aquifer and subsurface structures on North Cairo, Egypt, using integrated interpretation of magnetic, gravity, geoelectrical and geochemical data. *International Journal,***192**:94–112.

Sultan, A. Araffa, M., Hassan Saleh Sabet and Mustafa., Takey, S. (2019). Geophysical interpretation for groundwater exploration around Hurghada area.*Egypt Journal of Astronomy and Geophysics.***8**:171–179.

Tamriu Alemaayhu (2006). Hydrochemical and lake level changes in the Ethiopian rift, *Journal of Hydrology*, **14**: 15-62.

Telford, W. M., Geldart, L. Sheriff, R. E. (1990). Applied Geophysics: 2nd ed., Cambridge University Press. London, **20 (**5):453-461.

Tenalem Ayenew (2001). Numerical Groundwater flow modeling of the Central Main Ethiopian Rift lakes basin, *SINET Ethiopia J, Sci*., **24**(2):167-184.

Tenalam Ayenew (2008). Hydrogeological framework and occurrence of groundwater in the Ethiopian aquifers. *J. African Earth Sci.*, **52**:97-113.

Troisi, S., Fallicos, C., Straface, S. and Migliari, E. (2000). Application of kriging with external drift to estimate hydraulic conductivity from electrical resistivity data in unconsolidated deposits near Montato Uffugo, Italy, *Hydrogeol. Journal*, **8**: 356-367.

Tsegaye Abebe, Balestrieri, M.L. and Bigazzi, G. (2010). The Central Main Ethiopian Rift is younger than 8 Ma: Confirmation through apatite fission – track thermo-chronology, Terra Nova, **22**: 470–476.

Vijith, H. (2007). Groundwater potential in the hard rock terrain of Western Ghats: A case study from Kottayam district, Kerala using resource sat data and GIS techniques. *Jour. of the Indian Society of Remote Sensing*, **35**(2):163-171.

Yadav, G.S. and Abolfazli, H. (1998). Geoelectric soundings and their relationship to hydraulic parameters in semiarid regions of Jalore, northwestern India, *J. Applied Geophysics*, **39**:35-51.

Yechieli, Y. (2002). Fresh-saline ground water interface in the western Dead Sea area. *Indian J. of hydrol.Groundwater resource*, **38**: 615-623.

Young, M.E., de Bruijin, R.G.M. and Al-Ismaily, S. (1998). Reports: exploration of an alluvial aquifer in Oman by time-domain electromagnetic sounding. *Hydrogeol. J.*, **63**:83-393.

Yousef, A.F. (2008). The impact of North West active fault system on the recharge of the quaternary aquifer system around the Nile valley: case study Wadi El-Assiuti, Eastern Desert. Egypt. *European Water resource*, **21**:41–55.

Yousef, A. Narasimha, N.and Prasad, B. (2015). Delineation of Groundwater Potential Zones inDeep Midland Aquifers along Bharathapuzha River Basin, Kerala using Geophysical Methods, Cochin University of Science and Technology, Lakeside Campus, India, *marine geology and geophysics***, 4**:1039 – 1046.

Zohdy, A. R., Eaton, G. and Mabey, D. R. (1974). Application of surface geophysics to groundwater investigation. USGS publications. 116 pp.

Zohdy, A. R. (1969). The Use of Schlumberger and Eqatorial Soundings in Groundwater Investigations near El Paso, Texas. *Geophysics*, **34**:713-728.

APPENDICES

Annex 1: Interpreted VES curves.

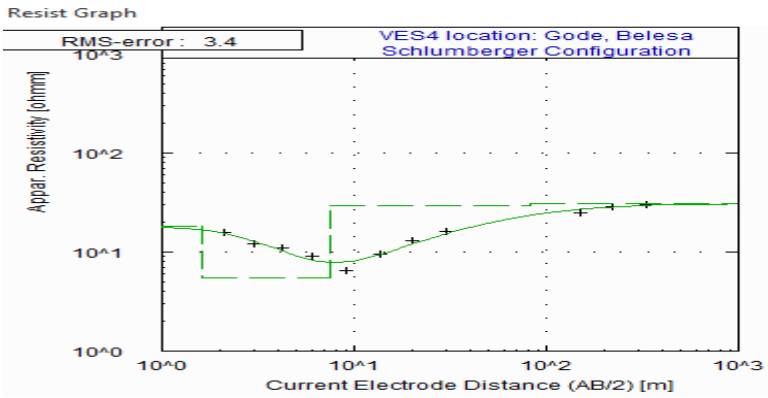

No	Res	Thick	Depth
1	18.4	1.6	1.6
2	5.6	5.8	7.5
3	29.6	75.3	82.7
4	30.7	-.-	-.-

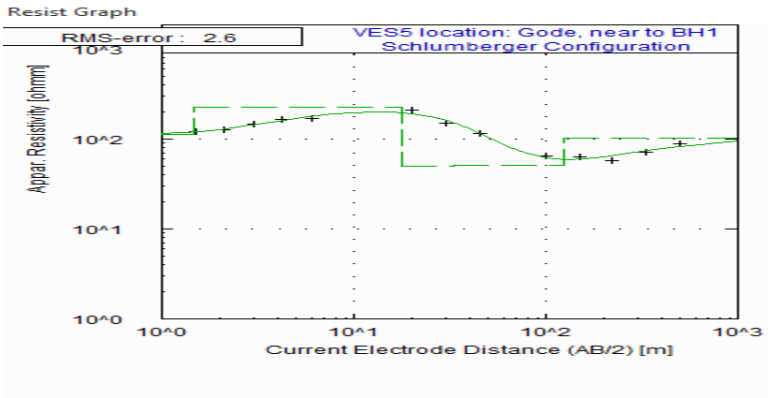

No	Res	Thick	Depth
1	114.0	1.5	1.5
2	228.6	16.1	17.6
3	50.2	15.2	32.8
4	51.0	90.0	122.8
5	101.9	-.-	-.-

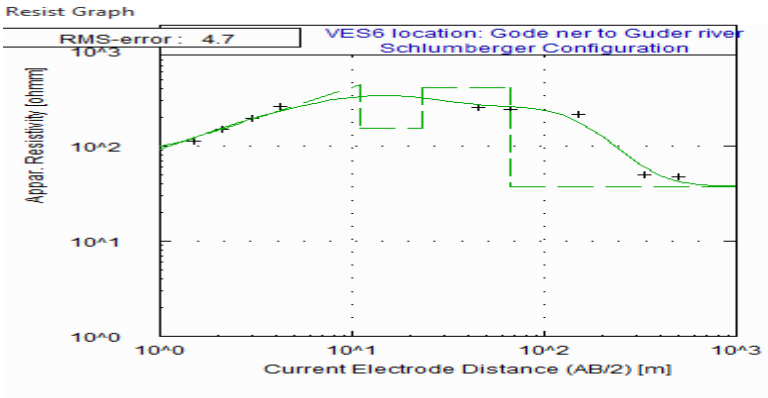

No	Res	Thick	Depth
1	79.8	0.8	0.8
2	440.7	10.1	10.9
3	154.0	12.3	23.2
4	407.2	43.8	67.0
5	37.2	-.-	-.-

Resist Graph

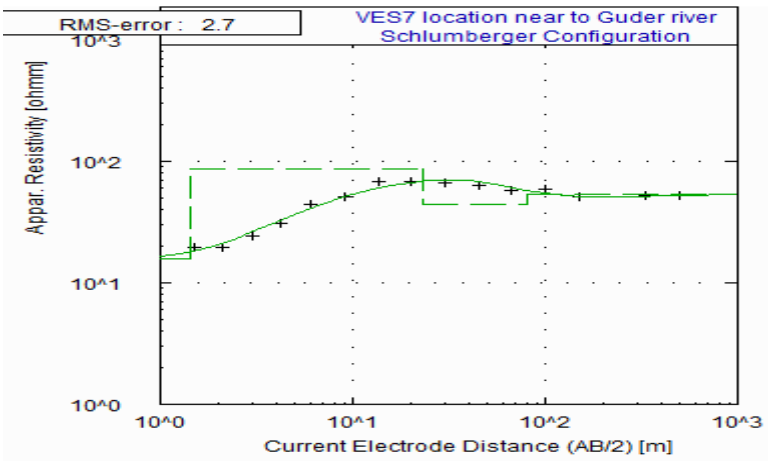

No	Res	Thick	Depth
1	15.8	1.4	1.4
2	85.7	21.5	23.0
3	43.8	58.4	81.4
4	53.6	-.-	-.-

Resist Graph

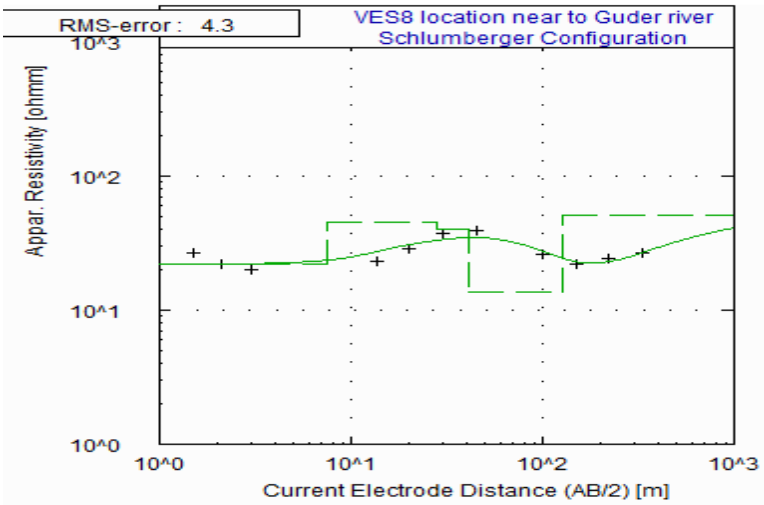

No	Res	Thick	Depth
1	22.1	7.5	7.5
2	45.4	20.6	28.1
3	39.9	13.6	41.6
4	13.5	86.2	127.8
5	50.8	-.-	-.-

Resist Graph

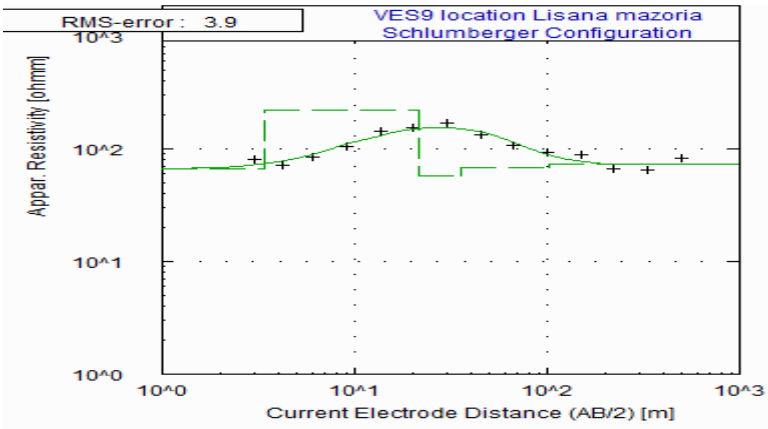

No	Res	Thick	Depth
1	66.7	3.4	3.4
2	221.7	18.3	21.8
3	58.1	13.8	35.6
4	68.8	65.8	101.4
5	73.8	-.-	-.-

Resist Graph

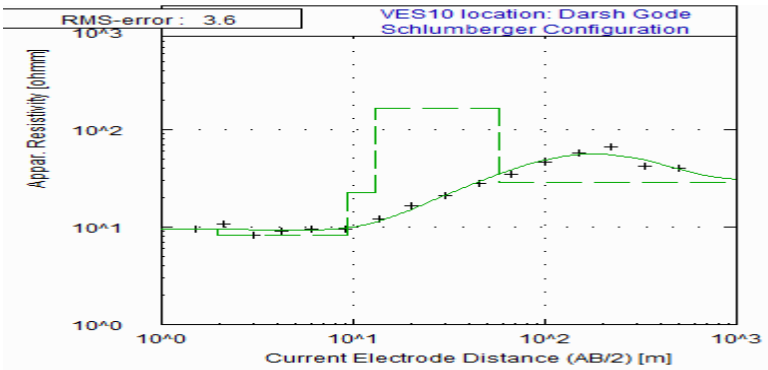

No	Res	Thick	Depth
1	9.6	2.0	2.0
2	8.3	7.3	9.2
3	22.6	3.9	13.1
4	165.5	44.3	57.4
5	28.8	-.-	-.-

Resist Graph

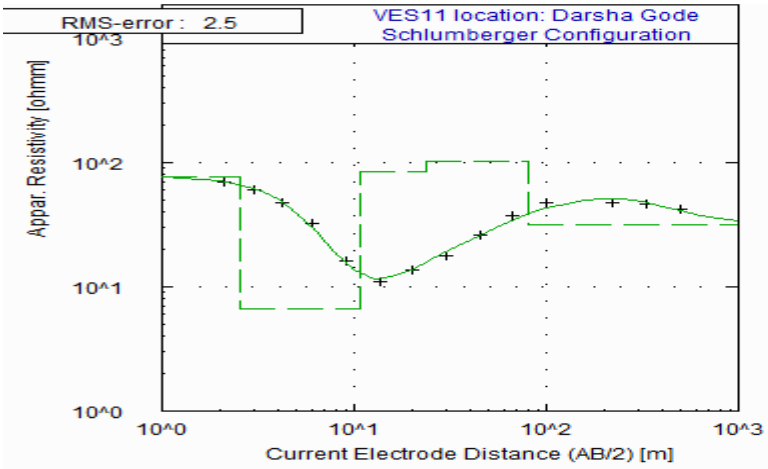

No	Res	Thick	Depth
1	76.8	2.5	2.5
2	6.7	8.3	10.9
3	84.0	12.7	23.6
4	102.8	56.1	79.7
5	31.8	-.-	-.-

Resist Graph

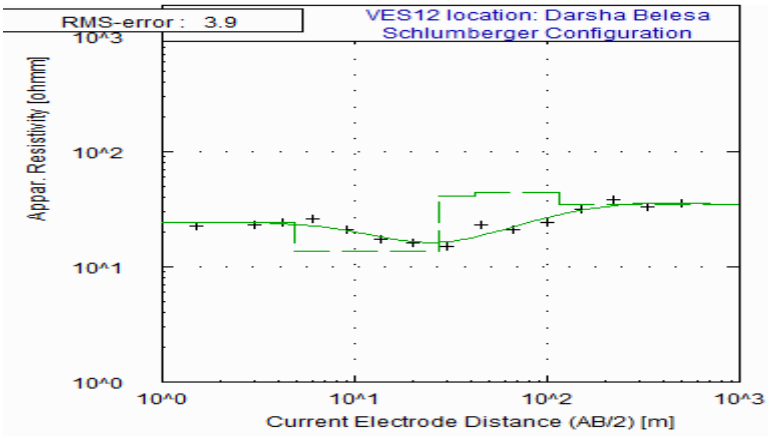

No	Res	Thick	Depth
1	24.5	4.9	4.9
2	13.7	22.6	27.5
3	41.4	15.0	42.6
4	44.7	72.4	115.0
5	34.4	-.-	-.-

Annex 2: Boreholes and description of lithologies over the study area